OSR 45-11(Rev 10-22-2008)

Savannah River Site

Supplier Document Status

- [x] 1.Work May Proceed
- [ ] 2.Submit Final Document - Work may proceed
- [ ] 3.Revise and Resubmit - Work may proceed subject to Resolution of Comments
- [ ] 4.Revise and Resubmit. Work may not Proceed.
- [ ] 5.Permission to proceed is not required.

Permission to proceed does not constitute acceptance or approval of design details, calculations, test methods, analysis or materials developed or selected by the supplier, and does not relieve supplier from full compliance with contractual obligations or release of any 'holds' placed on the contract.

Document ID	Revision
SRRA099188-000005	**A**

Document Category	Date
8-ANALYSIS AND DESIGN REPORTS	**2018-11-06 07:37:13 AM, EST**

Reviewer
KINARD, TIFFANY BROOKE

Contaminant Leaching from Saltstone Simulants for FY 2018

By

J.C. Seaman*, F.M. Coutelot**, and R.J. Thomas

*Senior Research Scientist
Assistant Director – Research/Quality Assurance
Savannah River Ecology Laboratory
The University of Georgia
Aiken, SC 29802
Phone: 803-725-0977
seaman@srel.uga.edu

**Assistant Research Scientist
coutelot@uga.edu

REVIEWS AND APPROVALS

Authors:

11/5/2018

John C. Seaman, SREL Associate Director-Research Date
Senior Research Scientist

Review:

11/5/2018

Matt R. Baker, SREL Date
Research Professional III

Approval:

11/5/2018

Jeremiah Mangold – SRR Technical Representative Date

Table of Contents

1.0 Executive Summary

At the Department of Energy's Savannah River Site (SRS) chemically reducing materials, such as blast furnace slag (BFS), are added to grout formulations containing ordinary portland cement (OPC) and fly ash (FA) and combined with low-level radioactive salt waste solutions in order to enhance the attenuation of redox sensitive contaminants (e.g., technetium-99 (^{99}Tc)). The resulting cementitious material, known as *Saltstone,* is deposited in a series of concrete vaults for long-term disposal at the Saltstone Disposal Facility (SDF). Once in place, saltstone provides both a physical (i.e., low saturated hydraulic conductivities (K_{sat}) that limit H_2O turnover and O_2 exposure) and a chemical barrier (i.e., residual reductive capacity) to contaminant release. However, the ability of cementitious materials to retain entrained contaminants is often evaluated using ground materials as sorbents, a practice that is likely to reduce the moisture level in the material, expose new reactive surfaces and soluble constituents, enhance exposure to O_2 that may facilitate changes in redox status and alter sorbent properties in an unpredictable manner. Therefore, the current objective was to evaluate contaminant partitioning and retention using intact saltstone materials that better mimic conditions within the disposal vaults.

The current report focuses on documenting saltstone simulant samples that were created for current and future testing, as well as results from ongoing tests concerning both ^{99}Tc and ^{129}I, the major risk drivers controlling long-term saltstone disposition. Current tests focused on evaluating the impact of changes in source materials (i.e., Holcim vs Lehigh BFS), dry feed formulations (conventional and cement free grouts), and even salt waste composition on contaminant retention properties of saltstone. In Fiscal Year 2017 saltstone simulants containing either ^{99}Tc or ^{129}I were created for testing to alleviate analytical problems associated with quantifying the two low-energy beta emitters in the same samples. With this limitation addressed, a set of saltstone simulants containing both radionuclides were created in Fiscal Year 2018 for future testing.

Technetium-99 and ^{129}I-spiked saltstone simulants were produced utilizing SRR prescribed formulations and subjected to curing under controlled temperature and humidity conditions that mimic the curing environment within SDU Cell 2A. Spiked saltstone simulants were also compared to actual intact saltstone retrieved (cured in place for approximately 20 months) from SDF-SDU Cell 2A. In the current report, contaminant mass transfer rates for the ^{129}I spiked saltstone simulants were assessed using EPA Method 1315, *Mass Transfer Rates of Constituents in Monolithic or Compacted Granular Materials Using a Semi-Dynamic Tank Leaching Procedure*. The results were compared to similar tests for other SDF contaminants (i.e., cesium-137 (^{137}Cs), ^{99}Tc, and nitrate (NO_3^-)) derived from spiked saltstone simulants and the SDF-SDU Cell 2A samples.

Results from Method 1315 were also compared to a novel test method developed at the Savannah River Ecology Laboratory (SREL) known as the Dynamic Leaching Method (DLM). In the DLM method a flexible-wall permeameter cell is used to achieve saturated leaching through intact grout monoliths under an elevated hydraulic gradient in an effort to evaluate the persistence of reductive capacity and subsequent changes in contaminant partitioning that occur within intact saltstone monoliths. The composition of the chemical leachates from both tests are then analyzed in an effort to identify critical reactions and solid phases controlling contaminant partitioning through geochemical modeling.

For the EPA 1315 tests ^{129}I leaching rates from spiked saltstone monoliths were generally consistent with previous tests involving the SDF-SDU Cell 2A samples. Iodine-129 leaching was similar to that of NO_3^-, as indicated by high effective diffusivities (D_e) and low leachability indices ($i.e.,\ LI = -\log[D_e]$), with less retention than observed for ^{137}Cs and ^{99}Tc in both spiked simulants and the SDF-SDU Cell 2A samples. Iodine-129 leaching behavior was also consistent with previous reported values for Cast Stone grout, a very similar cementitious material being investigated for the disposal of salt waste materials at the Hanford facility.

For DLM testing, the current data set reflects the continued leaching of a ^{99}Tc-spiked sample described in Seaman (2015) and a SDU-2A sample. It also reflects four new samples under evaluation, two saltstone samples spiked with ^{129}I and two samples spiked with ^{99}Tc, all of which were created using the new Lehigh BFS source material and cured for at least six months prior to DLM testing. The two ^{129}I samples were tested to provide the first DLM leaching data for ^{129}I, and the ^{99}Tc samples were used to evaluate the impact of leachate residence time on contaminant leaching using the new modified DLM system that utilizes mechanical pumps to better control test flow rates.

For the two extended tests (i.e., sample SDU-2A and ^{99}Tc-spiked (2015)), contaminant leaching continued in a steady manner, with about 10% of the total ^{99}Tc being leached from the two saltstones and 20% of the ^{137}Cs from SDU-2A, compared to 60 to >90% of the NO_3^- for the ^{99}Tc-spiked and SDU-2A saltstone samples, respectively. Effluent pH values for all saltstone DLM tests tended to be at least one unit higher using the new measurement technique that reduced sample exposure to the atmosphere prior to measurement. While oxidation reduction potential (ORP) values were also lower as well, indicating lower redox conditions, the ORP values were still somewhat higher than expected given that effluent ^{99}Tc levels are generally consistent with the solubility for possible Tc(IV) solid phases, i.e., $TcO_2.2H_2O$ or $TcO_2.1.6H_2O$.

DLM tests for the two new ^{99}Tc spiked samples indicated that the mechanical pumps were able to establish a continuous, low flow rate at the pressures required for saltstone testing, with some limitations depending on the inherent K_{sat} of the test material and the limited confining pressures that ensure flow is through the sample. Using the mechanical pumps continuous flow at steady rates of ≈ 0.17 and 0.42 mL d^{-1} were established, which enabled us to evaluate the impact of leachate residence time on contaminant leaching. Similar leaching patterns and cumulative ^{99}Tc and NO_3^- levels as a function of total leachate volume were observed at the two inlet flow rates. Although ^{99}Tc levels in the leachates were somewhat higher than observed previously, only 15% of the ^{99}Tc has leached from the sample while NO_3^- recovery is greater than 90%, indicating very different retention mechanisms.

Iodine-129 leaching from the two test samples was quite similar despite differences in flow rate (i.e., ≈ 0.2 vs. 0.4 mL d^{-1}), with high effluent recoveries that are similar to that observed for NO_3^-. Having a well-known initial ^{129}I inventory made it possible to calculate in-tact saltstone partition coefficients (K_d) that are on the order of 0.5 mL g^{-1}.

List of Figures

List of Tables

List of Acronyms and Abbreviations

AGW	Artificial Groundwater
ANS	American Nuclear Society
ANSI	American National Standards Institute, Inc.
APHA	American Public Health Association
ASTM	American Society for Testing and Materials
BFS	Blast Furnace Slag
DIW	Deionized Water
DLM	Dynamic Leaching Method
DOE	Department of Energy
EPA	Environmental Protection Agency
ICP-MS	Inductively Coupled Plasma-Mass Spectrometer
Ksat	Saturated Hydraulic Conductivity
LI	Leachability Index
OPC	Ordinary Portland Cement
ORP	Oxidation Reduction Potential
PA	Performance Assessment
psi	per square inch
QA	Quality Assurance
QC	Quality Control
SD	Standard Deviation
SDF	Saltstone Disposal Facility
SDU	Saltstone Disposal Unit
SHC	Saturated Hydraulic Conductivity
SREL	Savannah River Ecology Laboratory
SRR	Savannah River Remediation LLC
SRS	Savannah River Site
TCLP	Toxic Characterization Leaching Procedure
UHP	Ultra-High Purity
USEPA	United States Environmental Protection Agency
VZP	Vadose Pore-Water Solution
w/cm	Water-to-Cementitious Material Ratio

2.0 Introduction

Reactivity and saturated hydraulic conductivity (SHC; K_{sat}) are important factors controlling the rate of weathering and stability of cementitious materials used for the long-term disposal of low-level radioactive wastes. At the Savannah River Site (SRS) chemically reducing materials, such as blast furnace slag (BFS), are added to saltstone grout formulations mixed with low-level radioactive saltwaste materials in order to enhance the attenuation of redox sensitive contaminants, e.g., technetium (^{99}Tc). The persistence of chemically reducing conditions within the grout is an important factor driving long-term risk potential in the Performance Assessment (PA) for the Saltstone Disposal Facility (SDF). The residual reductive capacity of saltstone materials is a function of the grout formulation (i.e., the type and amount of reductive components like BFS), curing conditions, and the degree to which subsequent exposure to dissolved O_2 is restricted, an obvious function of the material's SHC.

Several studies have demonstrated both the difficulty in reducing pertechnetate (TcO_4^-; i.e., Tc(VII)), the oxidized form of Tc, and the rapid oxidation of reduced Tc (i.e., Tc(IV)) when exposed to even moderate levels of O_2 (Cantrell and Williams, 2013; Kaplan et al., 2011; Kaplan et al., 2008; Almond et al., 2012; Lukens et al., 2005; Ochs et al., 2016). Many of the previous experiments associated with the ability of saltstone to reduce and immobilize Tc have been conducted using ground saltstone materials as sorbents, a practice that is likely to expose new surfaces to oxidation and alter sorbent properties in an unpredictable manner. In addition, controlled H_2 atmospheres have been used as a means of restricting O_2 exposure for studies evaluating contaminant partitioning despite the fact H_2 may serve as a general chemical reductant and may alter the redox speciation of the target contaminants (i.e., Tc, Cr, Pu, etc.) and other important chemical elements (i.e., Fe, Mn, etc.) in the presence and even absence of the test sorbent, i.e., soil, saltstone, etc.

The leaching potential of contaminants from solid waste, including "size-reduced" cementitious materials, has previously been evaluated using the batch extraction method defined in EPA Method 1311, *Toxicity Characteristic Leaching Procedure* (TCLP) (USEPA 1992). The TCLP method was designed to represent the leaching conditions present in a municipal waste landfill scenario. However, contaminant mass transport in monolithic materials is controlled by diffusion through the tortuous pore network combined with the aqueous phase partitioning reactions at the solid/solution interface (i.e., adsorption/desorption, precipitation/dissolution, complexation reactions, etc.).

To address such issues, the United States Environmental Protection Agency (USEPA; EPA for short) Method 1315, *Mass Transfer Rates of Constituents in Monolithic or Compacted Granular Materials Using a Semi-Dynamic Tank Leaching Procedure* (USEPA 2013), was developed for evaluating the leaching potential of contaminants found in cementitious materials (Garrabrants et al., 2014; Kosson et al., 2014; Serne et al., 2015). EPA Method 1315 is similar to American National Standards Institute, Inc./American Nuclear Society Method 16.1 (ANSI/ANS16.1), *Measurement of the Leachability of Solidified Low-Level Radioactive Wastes by a Short-Term Test Procedure* (ANS 2003), with the leaching intervals modified to accommodate a more complex interpretation of contaminant release mechanisms. However, both methods are seen as vast improvements over previous tests using

size-reduced materials that focus on equilibrium partitioning rather than the rate of contaminant release under physically realistic conditions.

As noted above, the physical structure of the saltstone material combined with maintaining a high degree of saturation serves as a barrier against exposure to O_2. Grinding saltstone for sorption/desorption tests, and even removal from high humidity environments, may facilitate contaminant oxidation and the consumption of saltstone's inherent reductive capacity. The current report focuses on documenting saltstone simulant samples that were created for current and future testing, as well as results from ongoing tests concerning both ^{99}Tc and ^{129}I, the major risk drivers controlling long-term saltstone disposition. Current tests focused on evaluating the impact of changes in source materials (i.e., Holcim vs Lehigh BFS), dry feed formulations (conventional and cement free grouts), and even salt waste composition on contaminant retention properties of saltstone.

3.0 Materials and Methods

3.1 ^{99}Tc and ^{129}I Spiked Saltstone Formulations for EPA 1315 and DLM Testing

A series of spiked and non-spiked saltstone simulants were created for various characterization efforts. Table 1 contains a summary of the available test batches that were created in both FY2017 and FY2018. The relative concentrations of ^{99}Tc and/or ^{129}I in the salt waste simulants (i.e., ≈ 2 x 10^4 pCi mL^{-1} ^{99}Tc; 15 pCi mL^{-1} ^{129}I) were consistent with the average concentrations of ^{99}Tc and ^{129}I in the Tank 50 feed waste at the SDF (Bannochie, 2012, 2014). The test grout samples were created using four dry-feed materials: (1) Type II Ordinary Portland Cement (Holcim US, Inc. Birmingham, AL 35221), (2) Class F fly ash (The SEFA Group, Inc. Lexington, SC 29073), and two different BFS source materials, (3) Grade 100/120 blast furnace slag (Holcim) that has been used in the past, and (4) the new source material, Grade 100/120 blast furnace slag (Lehigh).

Table 1. Inventory of spiked and non-spiked saltstone samples available for testing.

Labels	BFS Type	Material %			Spike Level	Salt Waste
Synthesized 4-12-17		BFS	FA	OPC		
FY17CL	Lehigh	45	45	10	Control	ARP-MCU
FY17CH	Holcim	45	45	10	Control	ARP-MCU
FY17LI	Lehigh	45	45	10	^{129}I 15 pCi mL^{-1}	ARP-MCU
FY17HI	Holcim	45	45	10	^{129}I 15 pCi mL^{-1}	ARP-MCU
Synthesized 6-20-17						
FY17TcL	Lehigh	45	45	10	^{99}Tc 19,000 Ci mL^{-1}	ARP-MCU
Synthesized 6-14-18						
FY18-45L-45-10C	Lehigh	45	45	10	Control	New SWPF
FY18-60L-40C	Lehigh	60	40		Control	New SWPF
FY18-45L-45-10TcI	Lehigh	45	45	10	^{99}Tc 19,000 Ci mL^{-1}; ^{129}I 15 pCi mL^{-1}	New SWPF
FY18-60L-40TcI	Lehigh	60	40		^{99}Tc 19,000 Ci mL^{-1}; ^{129}I 15 pCi mL^{-1}	New SWPF

BFS: Blast Furnace Slag
FA: Fly Ash
OPC: Ordinary Portland Cement

In addition to the new BFS source, two different salt waste simulant formulations were utilized to reflect changes in the general composition of Tank 50 waste, the "ARP-MCU" salt waste that SREL has routinely used in the past and the "New SWPF" formulation that more accurately reflect the current Tank 50 composition (Table 2). To create a given salt waste, all of the chemicals in Table 2, except for the NaOH solution, were combined with ≈ 0.6 L of deionized water (DIW) in multiple 1-L volumetric polycarbonate flasks depending on the total mass of saltstone being created. The NaOH was then added as a 50% solution. When required, the contaminant spike solution was added to the salt waste flasks just before making up the solution to its final volume. The required masses of the dry feed materials were weighed and mixed together in a single bucket. After thorough homogenization of the combined dry powders, the salt waste simulant solution was slowly added to the dry materials while mixing at 250 rpm for 20 minutes. The final water to dry materials ratio used for the current formulations was 0.6. After mixing, the saltstone slurries were poured into several 2" ID x 4" L plastic concrete molds and sealed with plastic lids for curing (Test Mark Industries, Inc.). The plastic concrete molds were then placed in a humidity-controlled curing oven (Model 6105, Caron Products & Services, Inc.) and heated according to the curing profile from SDU Cell 2B (Figure 1) (Simner, 2016).

Table 2. Composition of various salt waste simulant solutions.

Material	ARP-MCU[a] (moles/L)	New SWPF[b] (moles/L)
Sodium Hydroxide, 50 wt% NaOH	1.594 (1.378)*	2.391 (1.823)*
Sodium Nitrate, $NaNO_3$	3.159	1.475
Sodium Nitrite, $NaNO_2$	0.368	0.583
Sodium Carbonate, Na_2CO_3	0.176	0.262
Sodium Sulfate, Na_2SO_4	0.059	0.055
Aluminum Nitrate, $Al(NO_3)_3.9H_2O$	0.054	0.142
Sodium Phosphate, $Na_3PO_4.12H_2O$	0.012	0.004

*Free OH molarity based on Aluminum content of salt waste mixture.
The simulant salt solutions were chemically designed to represent the average salt solution present in Tank 50:
a) After being treated via the Actinide Removal Process (ARP) and Modular Caustic side solvent extraction Unit (MCU)
b) After undergoing treatment at the Salt Waste Processing Facility (SWPF)

Figure 1. Curing profile for Saltstone Disposal Unit (SDU) Cell 2B (10.5 ft height) (Simner, 2016).

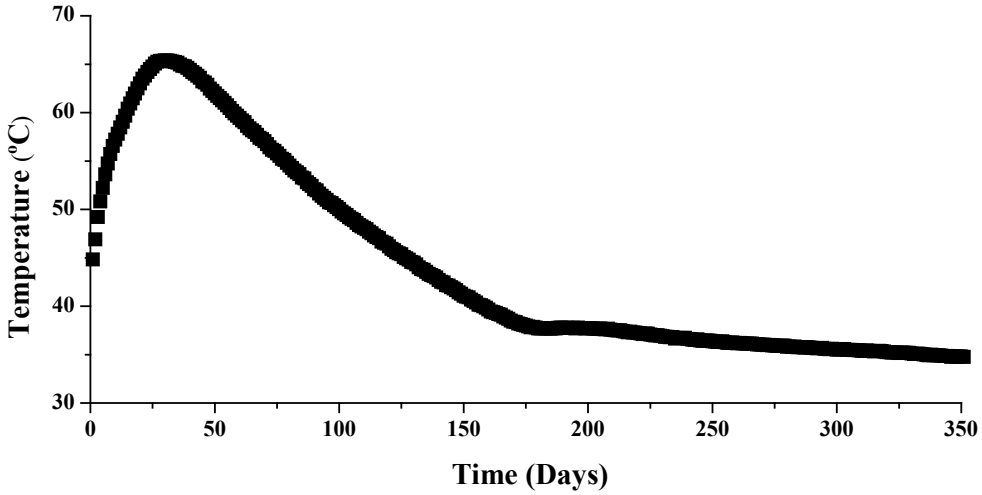

3.2 Contaminant Mass Transfer: EPA Method 1315: Mass Transfer Rates for Monolithic Samples

EPA Method 1315 was used to evaluate ^{129}I leaching from spiked samples that were created using either the Lehigh or Holcim BFS, i.e., FY17LI and FY17HI in Table 1. Prior to testing, the spiked samples were removed from the curing oven and sectioned to conform to the EPA 1315 Method recommendations. An artificial groundwater (AGW; see Table 3) surrogate based on routine sampling of non-impacted water table wells on the SRS was used as the leaching solution (Strom and Kaback, 1992). The mass transfer tests were conducted at room temperature (i.e., 22 ± 2 °C) under ambient laboratory atmosphere. Previous studies detailed in Seaman (2015) demonstrated that ^{99}Tc leaching from monolithic saltstone simulants was generally insensitive to the test atmosphere. The volume of eluent used in each leaching interval conformed to the liquid-to-surface area ratio (L/A) of 9 ± 1 mL cm^{-2}.

The pH and ORP of the leachant was recorded just prior to being replaced with fresh AGW solution according to the modified schedule provided in Table 4. Iodine-129 in the leachants was analyzed using low energy gamma analysis. At the same time, the EPA 1315 test was also performed using control saltstone samples without ^{129}I (i.e., samples FY17CH and FY17Cl in Table 1) to provide non-radioactive samples for additional chemical analysis. The leachant for these non-spiked samples was used for the analysis of NO_3^- by the chromotropic acid test method, *APHA Method-4500-Nitrogen, Standard Methods for the Examination of Water and Wastewater* (APHA, 1997), and major cations (i.e., Na, K, Mg, and Ca) by inductively coupled plasma-mass spectrometery (ICP-MS; NexION 300, Perkin Elmer Inc.) according to EPA Method 6020B Rev. 2 (USEPA 2014).

Table 3. Composition of the artificial groundwater (AGW) simulant.

Constituent/Parameter	AGW[a]
pH	5.0
	(mg L^{-1})
Na	1.39
K	0.21
Ca	1.00
Mg	0.66
Cl	5.51
SO_4	0.73

[a]Artificial Groundwater: non-impacted groundwater derived from natural infiltration (Strom and Kaback, 1992)

Table 4. Recommended schedule for fresh leachate renewals for EPA 1315, and actual sampling schedule used in testing ^{129}I spiked saltstone simulants, FY17HI (H45:45:10) and FY17LI (L45:45:10).

Interval	Duration (h)	Duration (d)	Cumulative Leaching Time (d)*	Actual (d)**
T01	2.0 ± 0.25		0.08	-
T02	23.0 ± 0.5		1	1
T03	23.0 ± 0.5		2	2
T04		5.0 ± 0.1	7	7
T05		7.0 ± 0.1	14	14
T06		14.0 ± 0.1	28	28
T07		14.0 ± 0.1	42	44
T08		7.0 ± 0.1	49	49
T09		14.0 ± 0.1	63	63

*Recommended versus **actual cumulative leaching durations

3.4 EPA 1315 Leachate Data Analysis

The effective diffusivity, D_e (cm^2 s^{-1}), for ^{129}I and NO_3^- was calculated using the simplified approach outlined in ANSI/ANS-16.1 (ANSI/ANS, 2003):

$$D_e = \pi \left[\frac{a_n / A_0}{\Delta t_n} \right] \left[\frac{V}{S} \right]^2 T \qquad [1]$$

where a_n is the quantity of contaminant released during interval n, A_0 is the total quantity of contaminant initially present in the sample being tested, Δt_n is the duration of the n^{th} interval, V is the volume of the sample (cm^3), S is the surface area of the sample (cm^2), and T is the generalized mean square root of the leaching time:

$$T = \left[\frac{\sqrt{t_n}+\sqrt{t_{n-1}}}{2}\right]^2 \quad [2]$$

where t_n is the elapsed time at the end of the current sampling interval and t_{n-1} is the elapsed time at the end of the previous sampling interval. The approach outlined above using the incremental fraction of the contaminant leached during each interval provides an estimate of diffusivity for each sampling interval that is independent of the other sampling intervals, and not subject to any bias that may occur during early sampling times when surficial materials may be released. When greater than 20% of the initial contaminant inventory has been leached from the sample, as is often seen for NO_3^-, the release data become non-linear with the square root of time due to depletion within the sample, and are not included in reported estimates of diffusivity (ANSI/ANS, 2003).

For comparison, the leachability index (LI), a unit-less parameter derived from the effective diffusion coefficient, i.e., D_e ($cm^2\ s^{-1}$), was calculated as follows:

$$LI_n = -\log[D_e] \quad [3]$$

where LI_n is the leachability index for sampling interval n (Serne et al., 2015). It is important to note that the "diffusional" release of retained contaminants from cementitious waste may reflect a combination of both chemical and physical transport processes, such as dissolution or desorption in response to changes in pore solution composition combined with diffusional transport. This complicates the mechanistic interpretation of leaching results.

3.5 Dynamic Leaching Method

Two versions of the Dynamic Leaching Method (DLM) test apparatus are displayed in Figure 2. DLM is based on ASTM D5084 for determining the SHC of cementitious materials using a flexible-wall permeameter to develop the necessary hydraulic gradient and ensure continuous internal flow. Darcy's Law was used to characterize the initial leaching conditions:

$$q = \frac{Q}{A} = \frac{K\Delta H}{L} \quad [4]$$

where q is the flux density (i.e., volume flowing through a specific cross-sectional area), Q ($cm^3\ sec^{-1}$) is the discharge volume per unit time (i.e., V/t), A is the cross sectional area (cm^2), K ($cm\ sec^{-1}$) is the hydraulic conductivity, ΔH is the hydraulic head difference between the column inlet and outlet (i.e., $\Delta H = H_i - H_o$; cm), and L is the length of the column (cm) (Hillel, 1980).

Given a two-inch diameter saltstone monolith (i.e., cross-sectional area of 20.27 cm^2) with a core length of one inch (2.54 cm), and an assumed SHC of 5 x 10^{-9} cm sec^{-1}, the pressure required to achieve a leaching rate of approximately 5 mL per day (i.e., 5.79 x 10^{-5} cm^3 sec^{-1}) can be calculated as:

$$q = \frac{Q}{A} = \frac{5.79\times10^{-5} cm^3 s^{-1}}{20.27\ cm^2} = 2.86 \times 10^{-6} cm\ s^{-1} = \frac{K\Delta H}{L} \quad [5]$$

The equation is then solved for ΔH, the required hydraulic gradient in cm.

$$\Delta H = \frac{qL}{K} = \frac{2.86\times10^{-6} cm\ s^{-1} L}{K} = \frac{2.86\times10^{-6} cm\ s^{-1}\times 2.54\ cm}{5\times10^{-9} cm\ s^{-1}} = 1453 cm \quad [6]$$

The hydraulic gradient is then converted to psi.

$$psi = \frac{1453 cm}{70.38\ cm\ psi^{-1}} = 20.61\ psi \quad [7]$$

Changes in the relative SHC during the course of leaching can be estimated using Darcy's equation based on the set hydrostatic pressure at the column inlet and the observed effluent flow rate, regardless of sample porosity. However, the porosity of each sample was determined by the mass loss of water upon heating samples to 105 °C in a laboratory oven, with samples measured repeatedly until the mass change on consecutive days was < 5% (Westsik et al., 2013). This was used as an estimate of sample Pore Volume (PV) for comparing sample monoliths of differing dimensions.

In Figure 2A, the driving pressure at the column inlet is a set compressed gas pressure controlled by a manual gas regulator, making it difficult to adjust and control the leaching rate, especially if the sample's SHC is changing. In Figure 2B, the leaching rate is controlled by a mechanical micro-pump, with changes in SHC indicated as a change in the back pressure on the pump.

Technetium-99 and ^{129}I present in the DLM leachates from spiked saltstone simulants was analyzed by liquid scintillation counting (LSC) according to ASTM D7283-13, *Standard Test Method for Alpha and Beta Activity in Water by Liquid Scintillation* (ASTM, 2013), using a Beckman/Coulter LS6500. The use of an internal standard was required for the DLM leachate due to sample quenching. Cesium-137 present in the leachates from the SDU-2A sample was determined by gamma spectrometry, while ^{99}Tc was measured by LSC. High levels of ^{137}Cs that complicated gamma analysis and beta energy overlap with ^{99}Tc precluded analysis of ^{129}I in the SDU sample leachates without extensive sample pre-treatment. Nitrate leaching for the saltstone samples was monitored using chromotropic acid test method noted above.

Figure 2. Diagram of the original DLM testing apparatus (2A) showing the flex-wall permeameter cell, inlet leachate source, and sample collection outlet. Revised DLM apparatus (2B) with mechanical pumps (Geocomp, Inc.) to provide stable, constant flow as back-pressures vary with continued leaching.

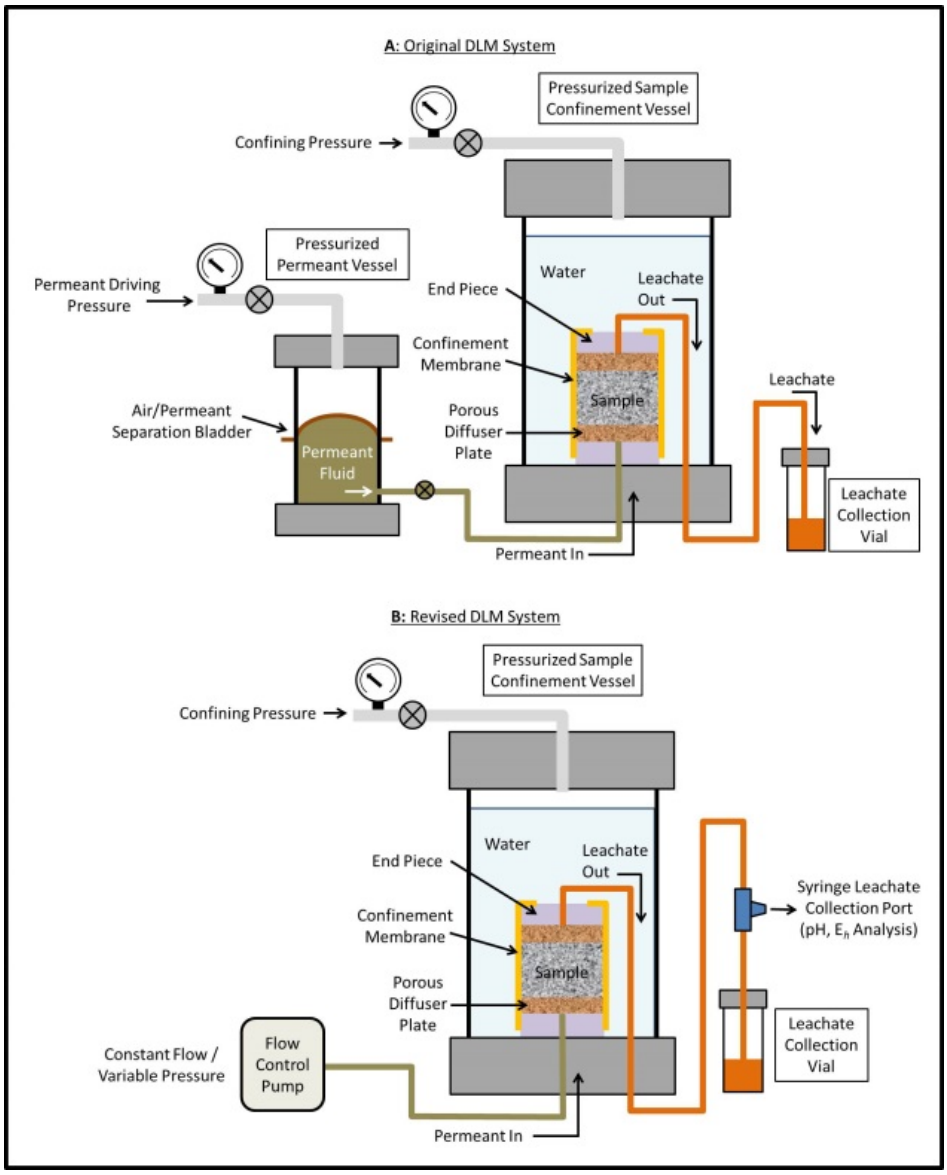

4.0 Results

4.1 EPA 1315 Results

The measured concentrations of ^{129}I in the EPA 1315 leachate from one of the ^{129}I spiked samples (i.e., FY17LI, see Table 1) and the three SDU Cell 2A samples are presented in Figure 3A, with the cumulative leaching fraction presented in Figure 3B. The EPA 1315 test was conducted using an FY17LI and an FY17HI sample that had been cured for approximately one month prior to testing. It is important to note that the ^{129}I levels in the leachate are quite low compared to the salt waste solution. Variations in the leaching pattern for the three SDU samples may be explained by changes in the Tank 50 feed solution that impact total ^{129}I in the sample. The average reported ^{129}I concentration in Tank 50 at the time these materials were poured, the third quarter of 2013, was 14.3 pCi mL^{-1} (Bannochie, 2014), with SRNL reporting an average ^{129}I concentration of 4.13 ± 0.88 pCi gm^{-1} for the SDU Cell 2A grout samples (Simner 2016, SRR-CWDA-2016-00051; Seaman and Coutelot, 2017), compared to 5.61 pCi gm^{-1} for the spiked simulants.

Figure 3. Leaching results for ^{129}I from EPA Method 1315 for a ^{129}I-spiked saltstone simulant FY17LI (L45:45:10) made with the ARP-MCU salt waste simulant and three SDU Cell 2A monoliths: (A) eluate concentration, (B) cumulative ^{129}I leaching.

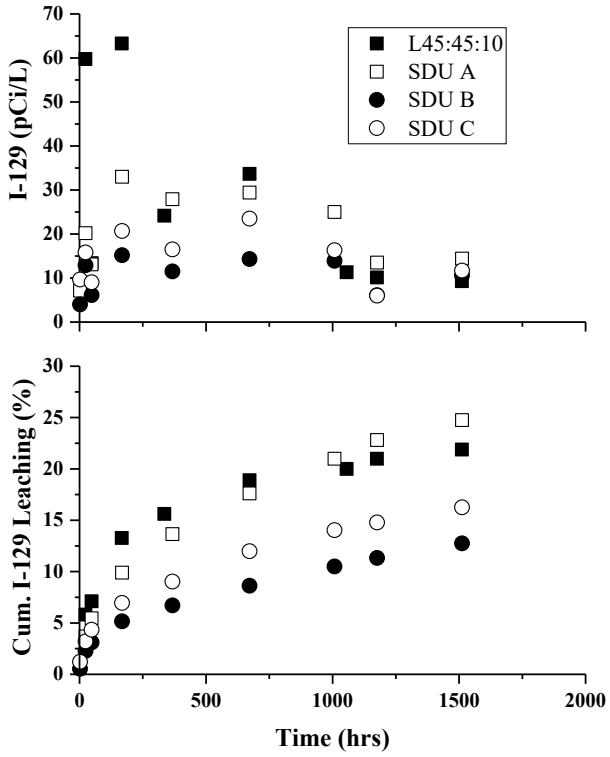

The measured concentrations of NO_3^- in the EPA 1315 leachate from one of the ^{129}I spiked samples (i.e., FY17LI) and the three SDU Cell 2A samples are presented in Figure 4A, with the cumulative leaching fraction for NO_3^- presented in Figure 4B. While the initial NO_3^- levels in the ^{129}I

spiked sample are somewhat higher than the three SDU Cell 2A samples, the cumulative fraction of NO_3^- leached is quite similar, reflecting the higher NO_3^- present in the "ARP-MCU" salt waste simulant compared to the Tank 50 waste at the time the SDU samples were poured.

Figure 4. Leaching results for NO_3^- from EPA Method 1315 for a ^{129}I-spiked saltstone simulant FY17LI (L45:45:10) made with the ARP-MCU salt waste and three SDU Cell 2A monoliths: (A) eluate concentration, (B) cumulative NO_3^- leaching.

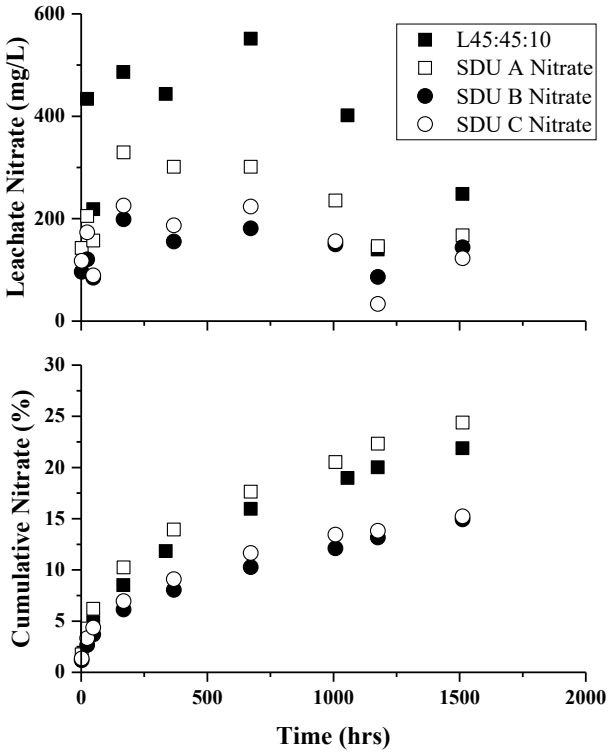

An updated summary of the data for all EPA leaching tests conducted by SREL is provided in Table 5 for comparison. Initial plots of the logarithm of cumulative release rate for ^{129}I and NO_3^- as a function of the logarithm of leaching time yield negative slopes of 0.5 ± 0.15, indicative of a "diffusion" controlled process (USEPA, 2013). However, when greater than 20% of the initial inventory of a specific contaminant has been leached from the sample, as was the case for ^{129}I and NO_3^-, the release generally no longer conforms to the diffusional model, and such data are not included in estimates of diffusivity or the leachability index, *LI*. At these later sampling intervals when the contaminant source within the monolith is depleted, the apparent diffusivity (D_e) decreases, which results in anomalously high LI values.

The LI range for the two spiked test samples, FY17HI and FY17LI, was 7.6 to 8.0, which is on the low end of the reported range for ^{129}I in the three SDU-2A samples, and similar to the range observed for NO_3^-. It is important to note that the test samples had only cured for about 1.5 months before analysis. After 91 days of curing, Westsik et al. (2013) reported effective diffusivities for I in Cast Stone monoliths that were in the range of 1 x 10^{-8} to 2 x 10^{-9} cm^2 s^{-1}, corresponding to LI values of 8 to 8.7. Westsik et

al. (2013) also reported a similar range of effective diffusivities for sodium (Na^+), NO_3^- and nitrite (NO_2^-), saltwaste constituents assumed to be poorly sorbed in cementitious grouts. Mattigod et al. (2011) also reported very limited retention of iodine in Cast Stone, with initial diffusivities that ranged from 1 x 10^{-7} cm^2 s^{-1} to ~3 x 10^{-7} cm^2 s^{-1} after 90 days of curing (LI ≈ 6.5 to 7.0), even lower than the current range.

In recent years, chemical getters, additives that help in immobilizing target contaminants, have been evaluated as a method to enhance the retention of ^{99}Tc and ^{129}I, the primary risk drivers for long-term disposal within cementitious material (Asmussen, et al., 2018; Qafoku et al. 2014). Such materials may be used to selectively remove the target contaminant from the liquid waste prior to the formation of grout or the material can be added to the liquid waste or the dry feed materials for eventual disposal as part of the final cementitious waste form. Qafoku et al. (2014) conducted extended batch tests focusing on five sequestering agents for ^{129}I, layered bismuth hydroxide (LBH), argentite mineral, synthetic argentite, silver-treated carbon, and silver-treated zeolite. Of the five, the synthetic argenite (Ag_2S) and the silver-treated zeolite were the most effective, with the remaining three showing limited effectiveness at the high pH and ionic strength of the simulated low activity waste. The effectiveness of argenite and silver-treated zeolite is due to the very limited solubility of silver iodide, AgI.

Table 5. Summary of effective diffusivities (D_e) and leachability indices (LI) derived from EPA 1315 (new data set highlighted in gray).

			^{99}Tc		Re		^{137}Cs		NO_3		^{129}I	
Sample	Curing Duration	Materials	D_e (cm^2/sec)	LI	D_e (cm^2/sec)	LI	D_e (cm^2/sec)	LI	D_e (cm^2/sec)	LI	D_e (cm^2/sec)	LI
FY18 Data												
FY17HI	1.5 Months	Old BFS (Holcim)	NA	NA	NA	NA	NA	NA	9.5E-08	7.0	2.8E-08	7.6
FY17LI	1.5 Months	New BFS (Lehigh)	NA	NA	NA	NA	NA	NA	8.2E-09	8.1	1.4E-08	8.0
FY15 Data*											^{127}I (stable iodine)	
	3 Months	Old BFS (Holcim)	2.4E-10	9.9	3.0E-08	7.6	NA	NA	4.4E-08	7.6	2.9E-08	7.7
	6 Months	Old BFS (Holcim)	2.8E-10	9.7	3.3E-08	7.6	NA	NA	1.6E-08	7.9	3.0E-08	7.7
			^{99}Tc		Re		^{137}Cs		NO_3		^{129}I	
FY16 Data												
Tc2	3 Months	New BFS (Lehigh)	2.6E-11	10.6	NA	NA	NA	NA	4.8E-08	7.5	NA	NA
Tc6	6 Months	New BFS (Lehigh)	5.7E-12	11.3	NA	NA	NA	NA	6.6E-08	7.2	NA	NA
Tc4 (1D)	6 Months	New BFS (Lehigh)	3.8E-11	10.4	NA	NA	NA	NA	2.1E-07	6.7	NA	NA
Tc9	3 Months	Old BFS (Holcim)	3.0E-10	9.6	NA	NA	NA	NA	3.7E-07	6.7	NA	NA
Sample A (SDU A)	20 Months**	Old BFS (Holcim)	6.4E-11	10.2	NA	NA	4.2E-10	9.4	1.3E-08	8.0	1.0E-08	8.0
Sample B (SDU B)	20 Months**	Old BFS (Holcim)	5.8E-11	10.3	NA	NA	1.1E-10	9.9	4.4E-09	8.5	2.5E-09	8.6
Sample C (SDU C)	20 Months**	Old BFS (Holcim)	5.2E-11	10.3	NA	NA	4.9E-10	9.3	5.5E-09	8.5	5.5E-09	8.4

*Reported in Seaman (2015). Reflects the average of three tests (1D configuration) in three different atmospheres

**20 months curing in SDU Cell 2A before sampling

NA Not Applicable

Sample A = SDU2A-0931-C-1-U-2

Sample B = SDU2A-0931-C-1-U-5

Sample C = SDU2A-0931-C-2-U-2

4.2 Dynamic Leaching Method – Tc-99

Previous reports have discussed ongoing tests aimed at evaluating contaminant partitioning within intact cementitious materials using the Dynamic Leaching Method (Seaman and Chang, 2014; Seaman et al., 2015, 2016, 2017). The DLM method uses a flexible-walled permeameter system to achieve steady saturated leaching through materials with relatively low saturated hydraulic conductivities, i.e., $K_{sat} \leq 1 \times 10^{-9}$ cm sec^{-1}. Seaman et al. (2015; 2016) first utilized the method to demonstrate that Re is a poor analogue for ^{99}Tc, with much greater Re leaching observed from intact samples, similar to the leaching pattern observed for NO_3^-.

The current report seeks to provide an update of ongoing leaching tests, summarize tests that have been terminated and document new leaching tests that were initiated in FY2018. Note that supplemental figures for DLM experiments conducted by SREL are provided in the Appendix. In FY2018, DLM testing for sample SDU-B (SDU2A-0931-C-2-U-2) was suspended because of the low hydraulic conductivity ($\leq 9 \times 10^{-11}$ cm sec^{-1}) of the sample, while DLM leaching for SDU-A (SDU2A-0931-C-1-U-2) continues. Although there were some initial differences in the ^{137}Cs leaching pattern for the two SDU samples (Figure 6), the cumulative effluent recovery is quite similar for as long as data for both is available, with effluent ^{137}Cs leveling off at about 20% of the total mass after leaching the SDU-A sample for 5+ pore volumes.

Figure 5. Effluent ^{137}Cs and cumulative ^{137}Cs recovery for the two SDU samples.

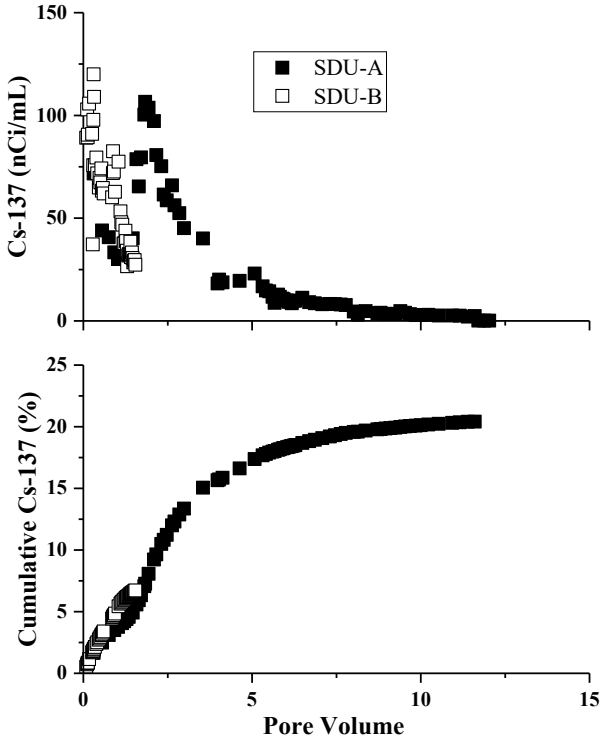

Effluent NO_3^- concentrations and the percentage of NO_3^- recovered in the effluent to date for SDU-A and the ^{99}Tc-spiked sample (Holcim 45:45:10) can be seen in Figure 6. For SDU-A, there appears to be some similarity between ^{137}Cs and NO_3^- with respect to the cumulative amount that can be leached from the sample. It is important to note, however, that the total fraction of ^{137}Cs that has been leached from the two SDU samples is much less than the cumulative NO_3^- levels, indicating some form of ^{137}Cs immobilization within the saltstone, consistent with the EPA 1315 leaching test results (Table 5). The *LI* values for ^{137}Cs ranged from 9.4 to 10 for three SDU samples while the *LI* values for NO_3^- in the SDU samples ranged 8.0 to 8.5.

Figure 6. Effluent NO_3^- and cumulative percent NO_3^- recovery for one SDU sample (SDU-A) and the ^{99}Tc-spiked sample (Holcim 45:45:10).

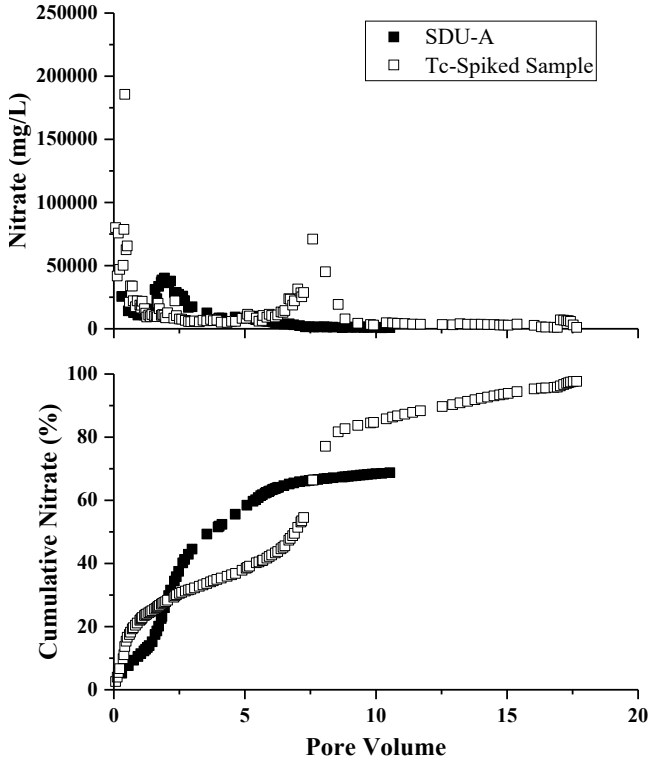

Figure 7 displays the effluent ^{99}Tc concentration and the cumulative effluent ^{99}Tc recovery for the SDU-A sample and the ^{99}Tc spiked sample (Holcim 45:45:10) for which NO_3^- leaching was illustrated in Figure 6. Although the leaching patterns are somewhat different for the two samples, a comparison with the NO_3^- and ^{99}Tc leaching patterns for the two samples clearly illustrates that ^{99}Tc is being retained to a greater degree within the saltstone. Using a similar leaching system at much higher pressures, Dinwiddie and Pickett reported similar effluent ^{99}Tc levels from an intact, spiked saltstone sample (Dinwiddie and Pickett, 2017).

Figure 7. Effluent ^{99}Tc and cumulative percent ^{99}Tc recovery for SDU-A sample and the ^{99}Tc-spiked sample (Holcim 45:45:10).

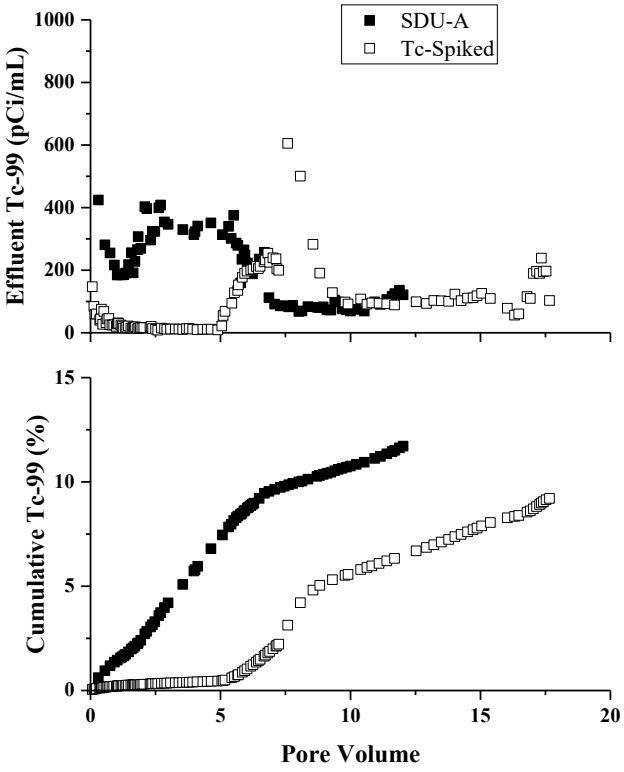

Difficulties in maintaining steady, continuous flow based on inlet pressure can complicate the interpretation of leaching results because of different leachate residence times depending on the materials inherent K_{sat}. This is further complicated by the reduction in K_{sat} that generally coincides with continued DLM leaching. In addition, transient spikes in contaminant leaching, like the coincidental effluent spike in NO_3^- (Figure 6) and ^{99}Tc (Figure 7) for the Tc-spiked sample (Holcim 45:45:10) that occurs around 7.5 pore volumes, may be attributed to an interruption in flow if the driving pressure changes dramatically. Even though the effluent spike is evident for both constituents, suggesting some change in physical conditions, the vast difference in total recovery suggests different mechanisms of sorption within the saltstone.

To address such limitations, the DLM system was modified to include mechanical pumps with the ability to maintain constant flow at high back pressures (Figure 8). Multiple ^{99}Tc-spiked saltstone sections from the same saltstone batch (Table 1; FY17TcL) were mounted in flex-walled permeameters and saturated with AGW according to the protocols of ASTM D5084. These samples were cured for approximately three months prior to DLM testing. After saturation, constant flow (with inlet varying pressure) was initiated at different inlet flow rates as part of a controlled test to see the impact of solute residence time on the effluent ^{99}Tc concentration, as well as effluent pH and ORP, with samples being collected using the modified protocol that limits atmospheric exposure. Of four samples that were initially tested, continuous flow was only achieved in two samples, the results of

which are presented below. In the other cases, there was a failure to achieve significant back pressure that indicates leachate flow was bypassing the sample.

Figure 8. Modified DLM control manifold utilizing three programmable micro-pumps (left) to maintain a constant flow rate for three test samples regardless of the back pressure.

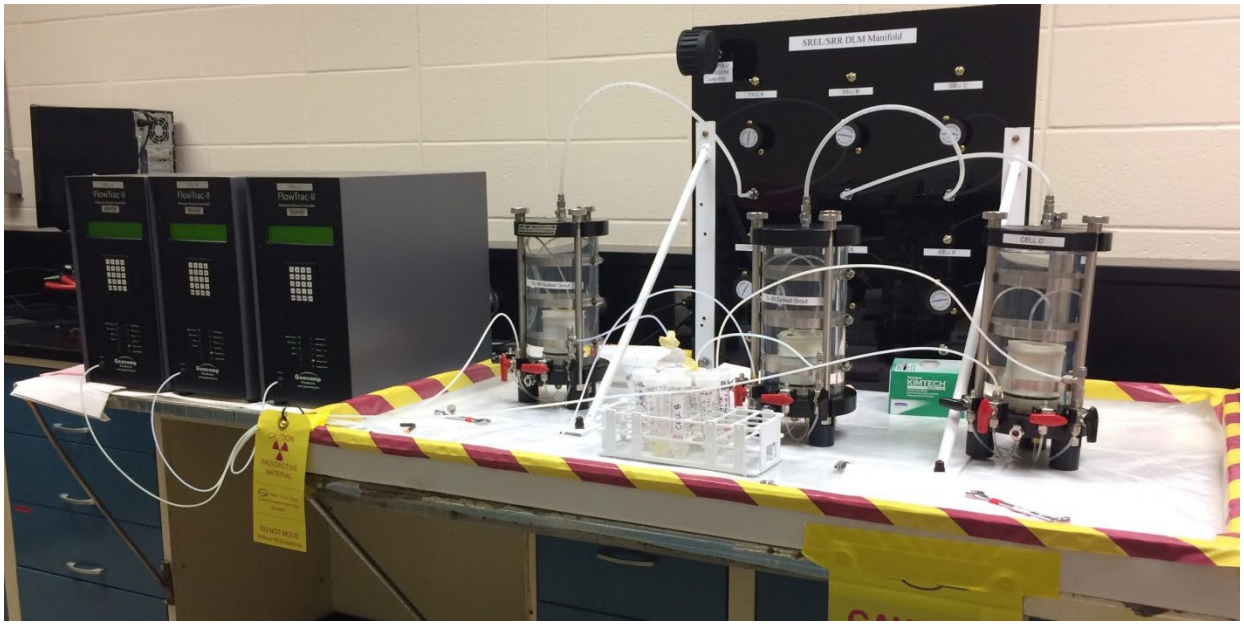

The ^{99}Tc and NO_3^- leaching patterns for two monoliths at different constant inlet flow rates are presented in Figure 10. Using the Geocomp. Inc. pumps continuous flow rates of 0.17 and 0.42 mL d^{-1} have been maintained for FY17TcL Sample A and Sample B, respectively. Despite somewhat higher ^{99}Tc levels than observed previously, the effluent concentrations (Figure 9A) and cumulative effluent totals (Figure 9C) are generally consistent for the two samples. The same is true for NO_3^- as well, with very similar effluent NO_3^- patterns despite the difference in leachate residence times (Figures 9B and 9D). Even though ^{99}Tc levels are somewhat higher than observed for the earlier DLM tests, the relative fraction of ^{99}Tc leached from the samples is much lower than observed for NO_3^-.

Figure 9. Effluent ^{99}Tc (A) and NO_3^- (B) plus cumulative percent ^{99}Tc (C) and NO_3^- (D) recovery ^{99}Tc-spiked saltstone samples made with Lehigh BFS (FY17TcL; Lehigh 45:45:10).

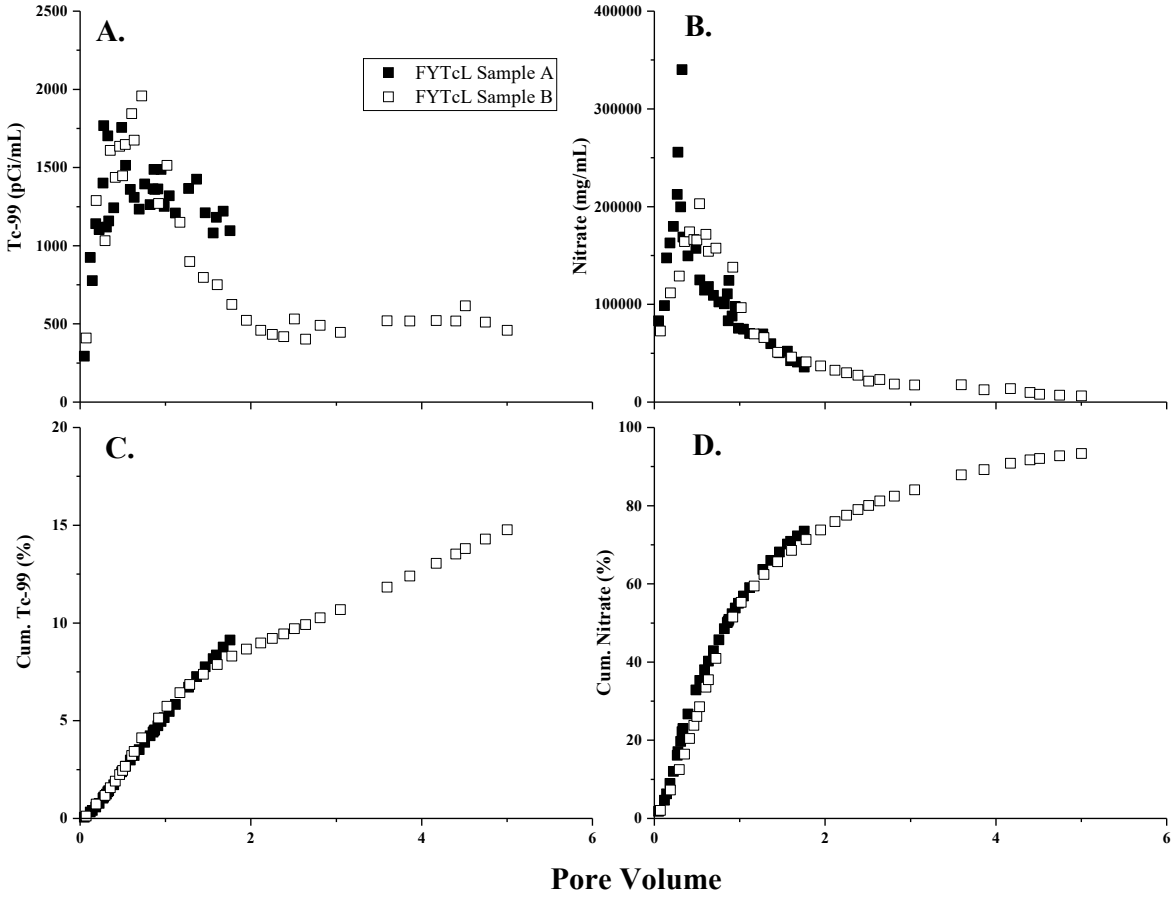

Figure 10 provides a graph of the solubility of two possible Tc(IV) solid phases that are thought to control ^{99}Tc partitioning in reducing grouts ((i.e., $TcO_2.2H_2O$ or $TcO_2.1.6H_2O$) as a function of pH at two different Eh values, -0.20 and -0.4 V. A more-thorough explanation of the modeling results is provided Seaman and Coutelot (2018; SREL R-18-004) All of the DLM data points for ^{99}Tc are then graphed as a function of pH. The data suggest that the Eh for pore solutions within the intact saltstone are likely within this range. Additional diagrams comparing DLM results to the solubility of various Tc(IV) solid phases as impacted by Eh values are included in the Appendix.

Figure 10. Solubility diagram for possible ^{99}Tc solid phases (i.e., $TcO_2.2H_2O$ or $TcO_2.1.6H_2O$) as a function of pH at two different Eh values, -0.2 and -0.4 V. Effluent data for ^{99}Tc DLM tests graphed as a function of sample pH.

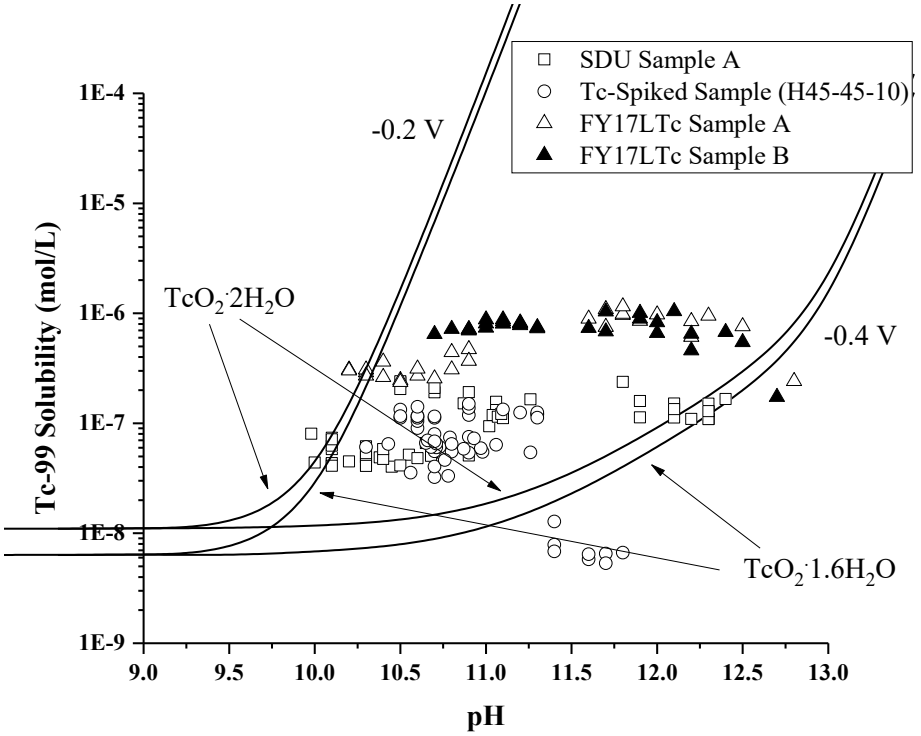

4.3 Dynamic Leaching Method – I-129

This is the first year that DLM results for ^{129}I are available as the high levels of ^{137}Cs present in the leachates from the SDU samples precluded ^{129}I analysis. Thus, a set of saltstone simulant samples were created that were only spiked with ^{129}I. Two of the ^{129}I-spiked samples made with Lehigh BFS (FY17LI; Lehigh 45:45:10, see Table 1) were mounted on the older pressure driven DLM system and leached continuously with AGW. The ^{129}I-spiked Sample A was cured for approximately six months and Sample B was cured for approximately thirteen months prior to the start of DLM testing. Iodine-129 leaching from the two test samples was quite similar despite differences in flow rate (i.e., ≈ 0.2 vs. 0.4 mL d^{-1}) and the length of curing, with high effluent recoveries that are similar to that observed for NO_3^-. Having a well-known initial ^{129}I inventory made it possible to calculate intact saltstone partition coefficients (K_d) that are on the order of 0.5 mL g^{-1} (Figure 11).

Figure 11. Effluent ^{129}I, cumulative percent ^{129}I recovery, and estimated saltstone Kd for spiked samples made with Lehigh BFS (FY17LI; Lehigh 45:45:10).

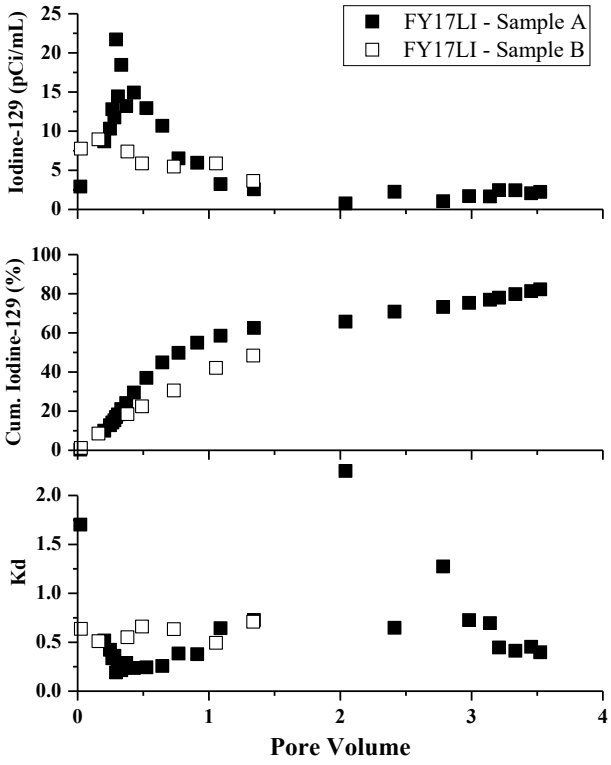

5.0 Discussion

The current report documents saltstone simulant samples that were created for current and future testing (including thermal testing reported in Seaman et al., 2018; SREL R-18-0005 Rev. 1.0), as well as results from ongoing tests concerning the immobilization of ^{99}Tc and ^{129}I. Current tests focused on evaluating the impact of changes in source materials (i.e., Holcim vs Lehigh BFS), dry feed formulations (conventional and OPC free grouts), and even salt waste composition on contaminant retention properties of saltstone.

Ongoing DLM experiments continued for ^{99}Tc-spiked saltstone simulants and samples from SDU Cell 2A. For the ^{99}Tc-spiked sample, ^{99}Tc leaching continued at a moderate level with cumulative totals that are far less than observed for NO_3^-, a poorly retained salt waste constituent. Results were consistent for the SDU sample in that ^{99}Tc was retained to a greater degree than ^{137}Cs, which was retained more than NO_3^-. These trends are consistent with previous EPA 1315 leaching tests for both spiked simulants and SDU samples.

A set of DLM leaching tests were initiated using the modified leaching system with mechanical pumps to control test flow rate. The objective was to evaluate the impact of pore water residence time on ^{99}Tc leaching. Technetium-99 spiked samples were leached at two flow rates, 0.17 and 0.42 mL d^{-1}. As observed previously, ^{99}Tc was retained to a greater degree than observed for NO_3^-. However, the cumulative leaching patterns for both ^{99}Tc and NO_3^- were not greatly impacted by flow rate, which suggests that retention mechanisms, although quite different for the two constituents, are not kinetically limited at the flow rates being evaluated. While equilibrium modeling efforts based on effluent pH and ^{99}Tc levels suggested that two possible Tc(IV) solid phases control ^{99}Tc retention for saltstone (i.e., $TcO_2{\cdot}2H_2O$ or $TcO_2{\cdot}1.6H_2O$), effluent Eh measurements were generally higher than expected. This suggests that current sampling methods fail to restrict O_2 exposure to effluent prior to Eh measurement at these low flow rates.

This report summarizes the first EPA 1315 and DLM test results for ^{129}I spiked saltstone simulants. Leaching rates from spiked saltstone monoliths were generally consistent with previous tests involving the SDF-SDU Cell 2A samples. Iodine-129 leaching was similar to that of NO_3^-, as indicated by high effective diffusivities (D_e) and low leachability indices ($i.e.,\ LI = -\log[D_e]$), with less retention than observed for ^{137}Cs and ^{99}Tc in both spiked simulants and the SDF-SDU Cell 2A samples. DLM tests were consistent as well, with a significant amount of the total ^{129}I ($\approx 80\%$) leached within the first 5 pore volumes. Even so, the calculated K_d values for ^{129}I partitioning in saltstone were approximately 0.5 mL g^{-1}.

6.0 Acknowledgements

The author would like to acknowledge the assistance of J. Cochran and K. Price with completion of the laboratory studies and production of this report.

7.0 References

Almond, P.M., D.I. Kaplan, C.A. Langton, D.B. Stefanko, W.A. Spencer, A. Hatfield, and Y. Arai (2012) Method Evaluation and Field Sample Measurements for the Rate of Movement of the Oxidation Front in Saltstone. SRNL, Aiken, SC 29808.

Asmussen, R. M., Pearce, C. I., Miller, B. W., Lawter, A. R., Neeway, J. J., Lukens, W. W., Bowden, M. E., Miller, M. A., Buck, E. C., Serne, R. J., and Qafoku, N. P. (2018). Getters for improved technetium containment in cementitious waste forms. Journal of Hazardous Materials 341, 238-247.

Angus M.J., Glasser F.P. (1985) The chemical environment in cement matrices. Mat. Res. Soc. Symp. Proc. 50:547-556.

APHA (1997) Method-4500-Nitrogen. Standard Methods for the Examination of Water and Wastewater, Washington, DC 20005.

ASTM (1999) Standard Practice for Microwave Digestion of Industrial Furnace Feedstreams and Waste for Trace Element Analysis. West Conshohocken, PA 19428-2959.

ASTM () ASTM D7168:

ASTM (2013) ASTM D7283-13 Standard Test Method for Alpha and Beta Activity in Water by Liquid Scintillation, West Conshohocken, PA.

ASTM (2008) ASTM D6527: Test Method for Determining Unsaturated and Saturated Hydraulic Conductivity in Porous Media by Steady-State Centrifugation, West Conshohocken, PA 19428-2959.

ASTM (2010) ASTM D5084-10: Standard Test Methods for Measurement of Hydraulic Conductivity of Saturated Porous Materials Using a Flexible Wall Permeameter, ASTM International, West Conshohocken, PA 19428-2959.

ASTM (2006) ASTM D2434 – 68: Standard Test Method for Permeability of Granular Soils (Constant Head), ASTM International, West Conshohocken, PA 19428-2959.

Bannochie C.J. (2012) Results of the Third Quarter 2012 Tank 50 WAC Slurry Sample: Chemical and Radionuclide Contaminants, Savannah River National Laboratory, Aiken, SC 29808. SRNL-STI-2012-00621.

Bannochie, C. J. (2014). "Results of the Third Quarter 2013 Tank 50 WAC Slurry Sample: Chemical and Radionuclide Contaminants." Savannah River National Laboratory, Aiken, SC 29808.

Cantrell K.J., Williams B.D. (2013) Solubility control of technetium release from Saltstone by $TcO_2 \cdot xH_2O$. J. Nuclear Materials 437:424-431. DOI: http://dx.doi.org/10.1016/j.jnucmat.2013.02.049.

Cantrell K.J., Carroll K.C., Buck E.C., Neiner D., Geiszler K.N. (2013) Single-pass flow-through test elucidation of weathering behavior and evaluation of contaminant release models for Hanford tank residual radioactive waste. Applied Geochemistry 28:119-127.

Clesceri L.S., Greenberg A.E., Trussell R.R. (1989) Standard methods for the examination of water and wastewater American Public Health Association, Washington, DC.

Dickson J.O., Harsh J.B., Lukens W.W., Pierce E.M. (2015) Perrhenate incorporation into binary mixed sodalites: The role of anion size and implications for technetium-99 sequestration. Chemical Geology 395:138-143. DOI: http://dx.doi.org/10.1016/j.chemgeo.2014.12.009.

El-Kamash, A.M., Sami, N.M., and El-Dessouky, M.I. (2011). Leaching Behavior of ^{137}Cs and ^{60}Co Radionuclides from Stabilized Waste Matrices. International Journal of Environmental Engineering Science 2, 199-211.

Garrabrants, A.C., F. Sanchez, C. Gervais, P. Moszkowicz, and D.S. Kosson (2002) The effect of storage in an inert atmosphere on the release of inorganic constituents during intermittent wetting of a cement-based material. Journal of Hazardous Materials 91:159-185.

Garrabrants A.C., Kosson D.S., DeLapp R., van der Sloot H.A. (2014) Effect of coal combustion fly ash use in concrete on the mass transport release of constituents of potential concern. Chemosphere 103:131-139. DOI: http://dx.doi.org/10.1016/j.chemosphere.2013.11.048.

Golovich, E.C., S.V. Mattigod, MMV Snyder, L. Powers, G.A. Whyatt, and D.M. Wellman. 2014. Radionuclide Migration through Sediment and Concrete: 16 Years of Investigations. PNNL-23841, Pacific Northwest National Laboratory, Richland, WA.

Gong, W., Xu, H., and Pegg, I.L. (2015) Development of Cement-Free Saltstone Formulations – Phase 3. VSL-15R2890-1, Vitreous State Laboratory, The Catholic University of America, Washington, DC.

Harbour, J.P. and M.F. Williams (2010) Impact of Curing Temperature on the Saturated Liquid Permeability of Saltstone. Savannah River National Laboratory, Aiken, SC. SRNL-STI-2010-00745.

Icenhower J.P., Qafoku N.P., Zachara J.M., Martin W.J. (2010) The biogeochemistry of technetium: A review of the behavior of an artificial element in the natural environment. American Journal of Science 310:721-752.

Kabai E., Beyermann M., Seeger J., Savkin B.T., Stanglmaier S., Hiersche L. (2013) Separation technique for the determination of 99Tc in milk and dairy products in case of emergency. Applied Radiation and Isotopes 81:36-41. DOI: http://dx.doi.org/10.1016/j.apradiso.2013.03.031.

Kaplan D.I., Lilley M.S., Almond P.M., Powell B.A. (2011) Long-term Technetium Interactions with Reducing Cementitious Materials, Savannah River National Laboratory, Aiken, SC.

Kaplan D.I., Roberts K., Shine G., Grogan K., Fjeld R., Seaman J. (2008) Range and distribution of technetium Kd values in the SRS subsurface environment, SRNL, Aiken, SC. pp. 47p.

Kosson D.S., Garrabrants A.C., DeLapp R., van der Sloot H.A. (2014) pH-dependent leaching of constituents of potential concern from concrete materials containing coal combustion fly ash. Chemosphere 103:140-147. DOI: http://dx.doi.org/10.1016/j.chemosphere.2013.11.049.

Langton CA. 2014. Technetium Oxidation in Slag-based Sodium Salt Waste Forms Exposed to Water and Moist Hanford Soil. SRNL-STI-2014-00399 Rev 0. Savannah River National Laboratory, Aiken, SC.

Langton C.A., Almond P.M. (2013) Cast stone oxidation front evaluation: Preliminary results for samples exposed to moist air, SRNL-STI-2013-00541.

Lehto J., Hou X. (2011) Chemistry and Analysis of Radionuclides Wiley-VCH, Weinheim, Germany.

Lukens W.W., Bucher J.J., Shuh D.K., Edelstein N.M. (2005) Evolution of technetium speciation in reducing grout Environ. Sci. & Technol. 39:8064-8070.

Lukens W.W., McKeown D.A., Buechele A.C., Muller I.S., Shuh D.K., Pegg I.L. (2007) Dissimilar Behavior of Technetium and Rhenium in Borosilicate Waste Glass as Determined by X-ray Absorption Spectroscopy. Chemistry of Materials 19:559-566. DOI: 10.1021/cm0622001.

Lee W., Batchelor, B. (2003) Reductive capacity of natural reductants. Environ. Sci. Technol. 37:535-541.

Maset E.R., Sidhu S.H., Fisher A., Heydon A., Worsfold P.J., Cartwright A.J., Keith-Roach M.J. (2006) Effect of Organic Co-Contaminants on Technetium and Rhenium Speciation and Solubility under Reducing Conditions. Environmental Science & Technology 40:5472-5477. DOI: 10.1021/es061157f.

Mattigod, S. V., Westik, J. H., Chung, C. W., Lindberg, M. J., and Parker, K. E. (2011). "Waste Acceptance Testing of Secondary Waste Forms: Cast Stone, Ceramicrete and DuraLith." Pacific Noerthwaest National Laboratories. PNNL-20632.

McCloy J.S., Riley B.J., Goel A., Liezers M., Schweiger M.J., Rodriguez C.P., Hrma P., Kim D.S., Lukens W.W., Kruger A.A. (2012) Rhenium Solubility in borosilicate nuclear waste glass: Implications for the processing and immobilization of technetium-99. Environ. Sci. & Technol. 46:12616-12622.

Neeway J.J., N. Qafoku, R.J. Serne, A.R. Lawter, J.R. Stephenson, W.W. Lukens, and J.H. Westsik, Jr. (2014) Evaluation of Technetium Getters to Improve the Performance of Cast Stone. PNNL-23667, Pacific Northwest National Laboratory, Richland, WA.

Perkin Elmer Field Application Report, The Determination of Iodine in Food with the ELAN DRC-e ICP-MS (http://www.perkinelmer.com/Content/applicationnotes/far_iodineinfoodwithelandrc-e.pdf).

Pierce E.M., Lukens W.W., Fitts J.P., Jantzen C.M., Tang G. (2014) Experimental determination of the speciation, partitioning, and release of perrhenate as a chemical surrogate for pertechnetate from a sodalite-bearing multiphase ceramic waste form. Applied Geochemistry 42:47-59. DOI: http://dx.doi.org/10.1016/j.apgeochem.2013.12.017.

Roberts, K.A., and D.I. Kaplan (2009) Reduction Capacity of Saltstone and Saltstone Components. Savannah River National Laboratory, Aiken, SC, SRNL-STI-2009-00637.

Qafoku N., J.J. Neeway, A.R. Lawter, T.G. Levitskaia, R.J. Serne, J.H. Westsik, Jr, and M.M.V. Snyder (2015) Technetium and Iodine Getters to Improve Cast Stone Performance. PNNL-23282 Rev. 1, Pacific Northwest National Laboratory, Richland, WA.

Sayed, M. S., and Khattab, M. M. (2010). Immobilization of Liquid Radioactive Wastes by Hardened Blended Cement - White Sand Pastes. J. American Science 6, 334-341.

Serne, R.J., J.H. Westsik Jr., Williams B.D., Jung H.B., Wang G. (2015) Extended Leach Testing of Simulated LAW Cast Stone Monoliths, Pacific Northwest National Laboratory, PNNL-24297 RPT-SLAW-001 Rev 0, Richland, WA.

Seaman, J.C. and F.M. Coutelot (2018) Technetium Solubility in Saltstone as Function of pH and Eh: Summary of Modeling Efforts, SREL Doc. R-18-0004, ver. 1.0. Submitted to SRR August 16, 2018.

Seaman, J.C., F.M. Coutelot, and R.J. Thomas (2018) Thermal Properties of Saltstone Simulants, SREL Doc. R-18-0005, ver. 1.0. Submitted to SRR October 17, 2018.

Seaman, J.C., and F.M. Coutelot (2017) Contaminant Leaching from Saltstone, SREL Doc. R-17-0005, ver. 1.0. Submitted to SRR September 29, 2017.

Seaman, J.C., H.S. Chang, and S.W. Buettner. (2014) Chemical and Physical Properties of Saltstone as Impacted by Curing Duration, SREL Doc. R-14-0006, ver. 1.0. Submitted to SRR September 23, 2014.

Seaman, J.C., H.S. Chang, and S.W. Buettner. 2013. Comparison of Hydraulic Property Measurement Techniques for Simulated Saltstone. SREL Doc. R-13-0006, ver. 1.0. Submitted to SRR September 4, 2013.

Shu X., Shen L., Wei Y., Hua D. (2015) Synthesis of surface ion-imprinted magnetic microsphere for efficient sorption of perrhenate: A structural surrogate for pertechnetate. Journal of Molecular Liquids 211:621-627. DOI: http://dx.doi.org/10.1016/j.molliq.2015.07.059.

Simner, S. P. (2016). Property Data for Core Samples Extracted from SDU Cell 2A. Savannah River Remediation. SRR-CWDA-2016-00051.

Strom R.N., Kaback D.S. (1992) SRP Baseline Hydrogeologic Investigation: Aquifer Characterization Groundwater Geochemistry of the Savannah River Site and Vicinity (U), Westinghouse Savannah River Company, Environmental Sciences Section, Aiken, SC. pp. 98.

Stumm W., Morgan J.J. (1995) Aquatic chemistry: An introduction emphasizing chemical equilibria in natural waters. 3rd ed. Wiley-Interscience, New York.

Tagami K., Uchida S. (2004) Comparison of transfer and distribution of technetium and rhenium in radish plants from nutrient solution. Applied Radiation and Isotopes 61:1203-1210. DOI: http://dx.doi.org/10.1016/j.apradiso.2004.05.074.

USEPA. (1992) Method 1311: Toxicity Characteristic Leaching Procedure, Test Methods for Evaluating Solid Waste, Physical/Chemical Methods (SW-846), Office of Solid Waste, Washington, DC.

USEPA (1996) Method 3052, Rev. 0 Microwave assisted acid digestion of siliceous and organically based matrices. Test Methods for Evaluating Solid Waste, Physical/Chemical Methods (SW-846), Office of Solid Waste, Washington, DC.

USEPA (2007) Method 6020A, Rev. 1. Inductively coupled plasma-mass spectrometry, Test Methods for Evaluating Solid Waste, Physical/Chemical Methods (SW-846), Office of Solid Waste, Washington, DC.

USEPA (2013) Method 1315, Mass transfer rates of constituents in monolithic or compacted granular materials using a semi-dynamic tank leaching procedure. Test Methods for Evaluating Solid Waste, Physical/Chemical Methods (SW-846), Office of Solid Waste, Washington, DC.

Westsik J.H., Jr, G.F. Piepel, M.J. Lindberg, P.G. Heasler, T.M. Mercier, RL Russell, A. Cozzi, W.E. Daniel Jr, R.E. Eibling, E.K. Hansen, M.M. Reigel, and D.J. Swanberg. 2013. Supplemental Immobilization of Hanford Low-Activity Waste: Cast Stone Screening Tests. PNNL-22747, Pacific Northwest National Laboratory, Richland, WA.

Zheng, J., H. Takata, K. Tagami, T. Aono, K. Fujita, and S. Uchida. 2012. Rapid Determination of Total Iodine in Japanese Coastal Seawater using SF-ICP-MS. Microchemical J. 100:42-47.

8.0 Appendix

8.1 Tc Solubility Curves

8.1.1 *TcO_2·1.6(H_2O) Solubility Curves*

Figure 12. Solubility of TcO_2.1.6(H_2O)$_{(s)}$ as a function of Eh (Ideal Dilute Conditions) (all other Tc minerals suppressed) compared to various DLM results.

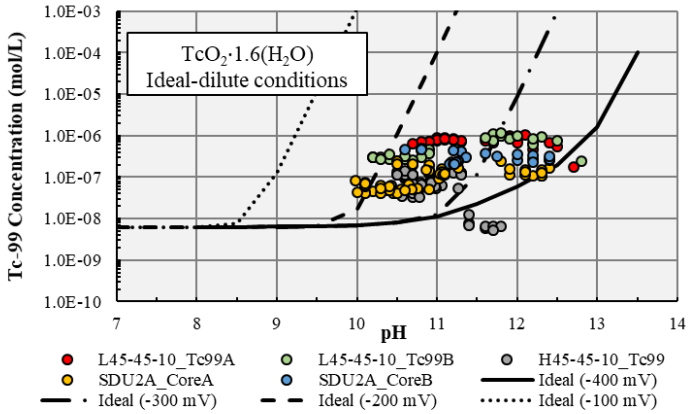

Figure 13. Solubility of TcO_2.1.6(H_2O)$_{(s)}$ as a function of Eh (1 PV DLM Conditions) (all other Tc minerals suppressed) compared to various DLM results.

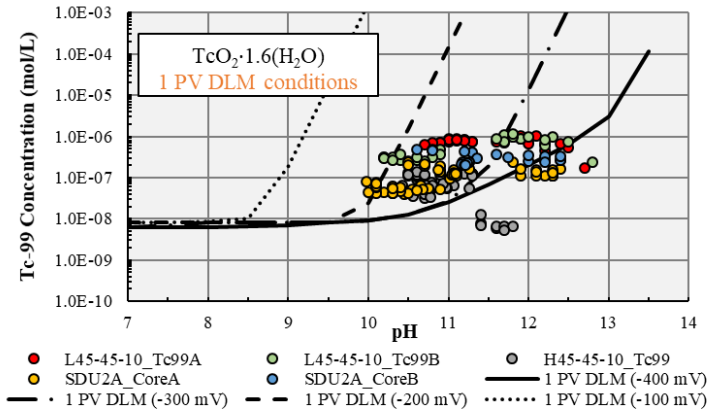

Figure 14. Solubility of TcO_2.1.6(H_2O)$_{(s)}$ as a function of Eh (5 PV DLM Conditions) (all other Tc minerals suppressed) compared to various DLM results.

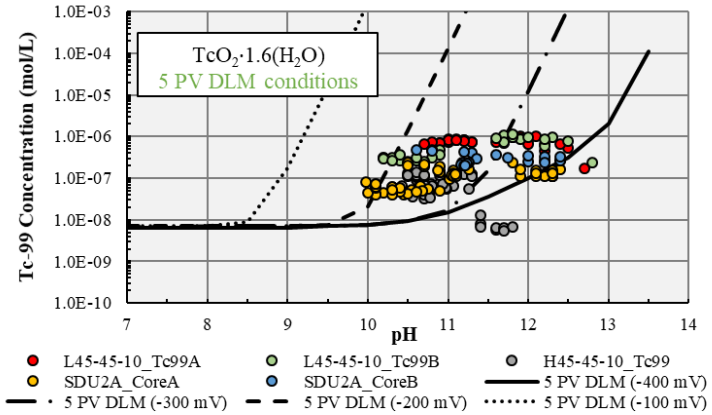

8.1.2 *$TcO_2 \cdot 2(H_2O)$ Solubility Curves*

Figure 15. Solubility of $TcO_2.2(H_2O)_{(s)}$ as a function of Eh (Ideal Dilute Conditions) (all other Tc minerals suppressed) compared to various DLM results.

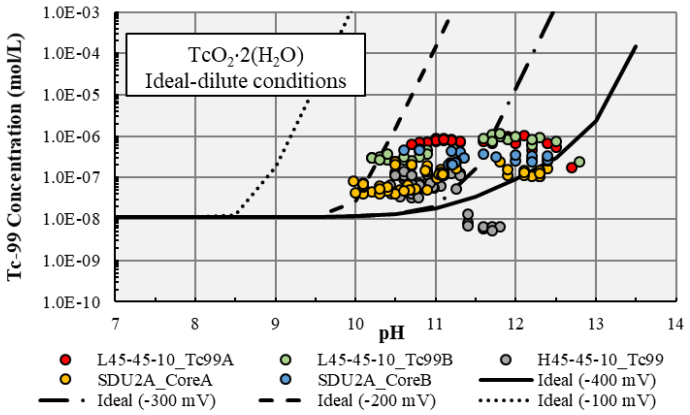

Figure 16. Solubility of $TcO_2.2(H_2O)_{(s)}$ as a function of Eh (1 PV DLM Conditions) (all other Tc minerals suppressed) compared to various DLM results.

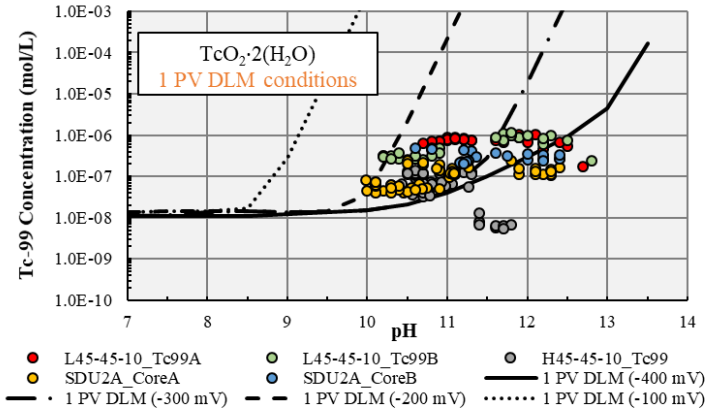

Figure 17. Solubility of $TcO_2.2(H_2O)_{(s)}$ as a function of Eh (5 PV DLM Conditions) (all other Tc minerals suppressed) compared to various DLM results.

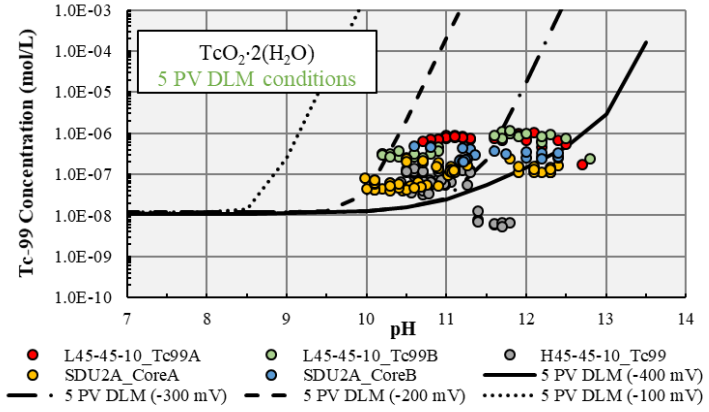

8.1.3 *TcO_2 Solubility Curves*

Figure 18. Solubility of $TcO_{2(s)}$ as a function of Eh (Ideal Dilute Conditions) (all other Tc minerals suppressed) compared to various DLM results.

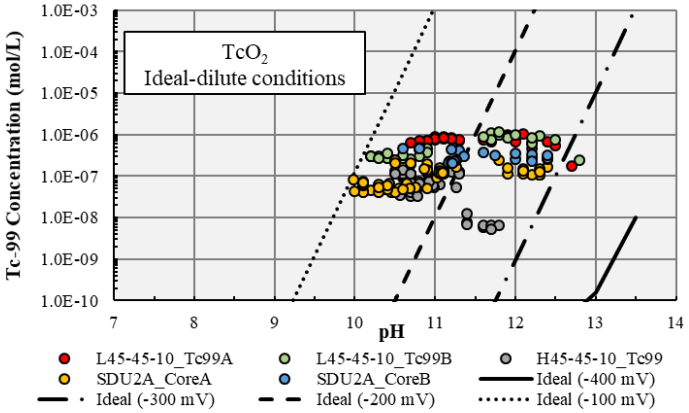

Figure 19. Solubility of $TcO_{2(s)}$ as a function of Eh (1 PV DLM Conditions) (all other Tc minerals suppressed) compared to various DLM results.

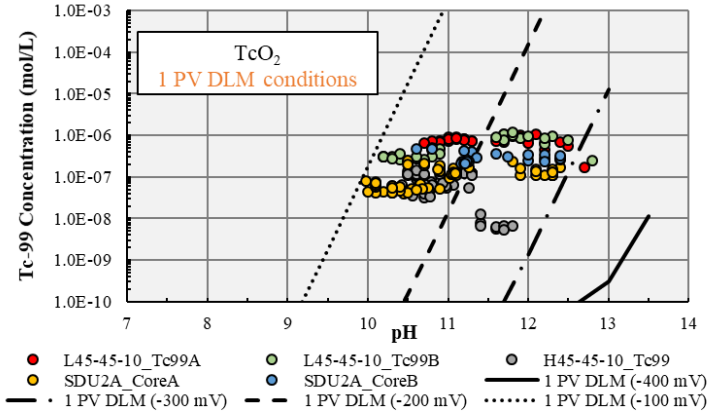

Figure 20. Solubility of $TcO_{2(s)}$ as a function of Eh (5 PV DLM Conditions) (all other Tc minerals suppressed) compared to various DLM results.

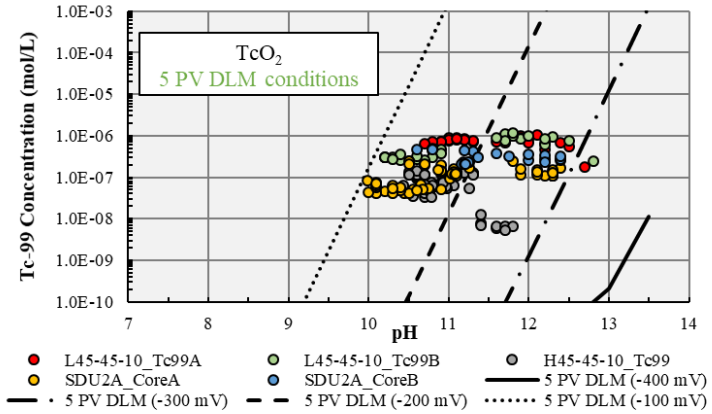

8.2 Supplemental DLM Figures

In the following figures note that:

L45-45-10_Tc99X where X = A or B, are the FY17TcL samples found in Table 1.

H45-45-10_Tc99 is a DLM experiment conducted using a 45-45-10 dry mix of BFS (Holcim), FA, and OPC, respectively. The ARP-MCU salt solution simulant was used in synthesizing this saltstone simulant and contained a Tc-99 concentration of 20,000 pCi/mL.

SDU2A_CoreX where X = A or B, are actual field samples taken from SDU 2A that are being used for DLM experiments.

L45-45-10_I129X where X = A or B, are the FY17LI samples found in Table 1.

8.2.1 *Tc-99 DLM Experiments*

Figure 21. DLM effluent concentrations of Tc-99 vs. pore volume exchanges

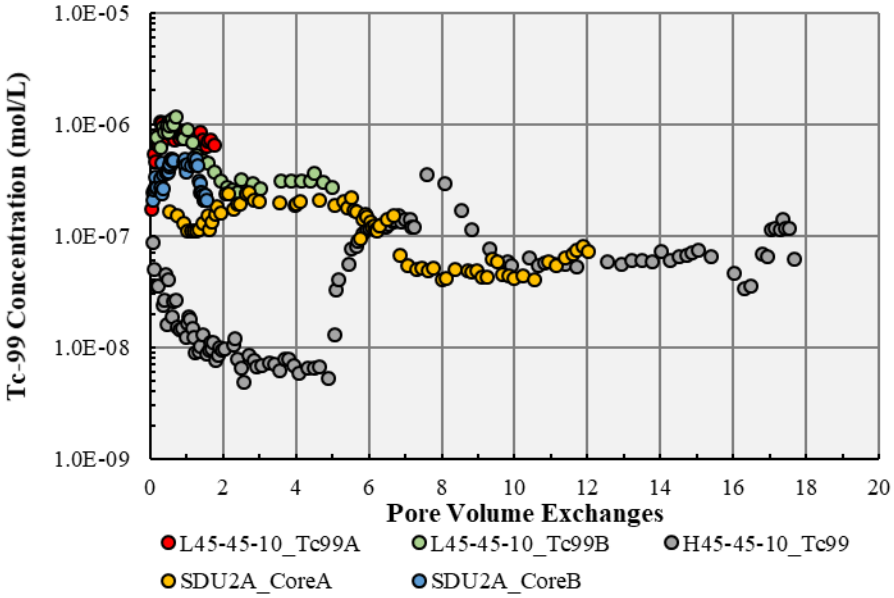

Figure 22. Cumulative percent Tc-99 released from DLM effluent

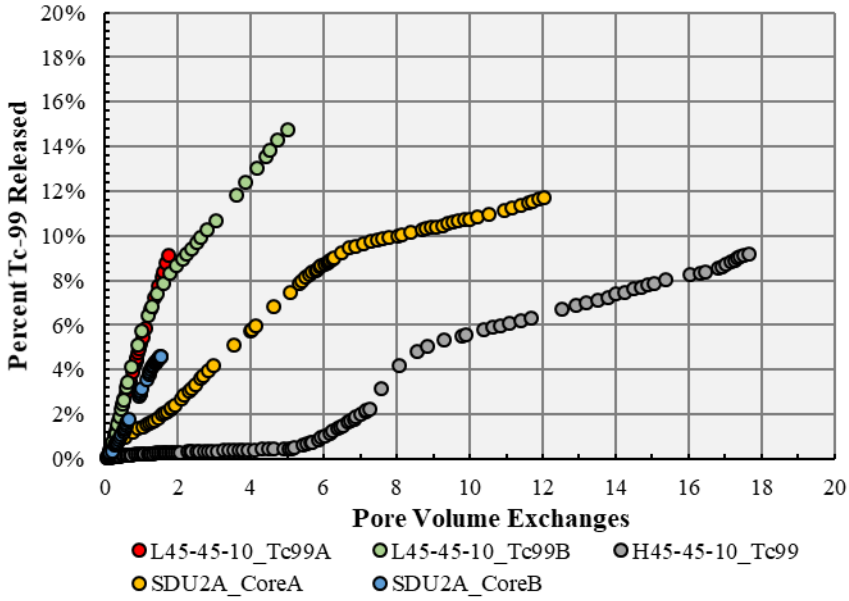

Figure 23. DLM effluent concentrations of nitrate (NO_3^-) vs. pore volume exchanges

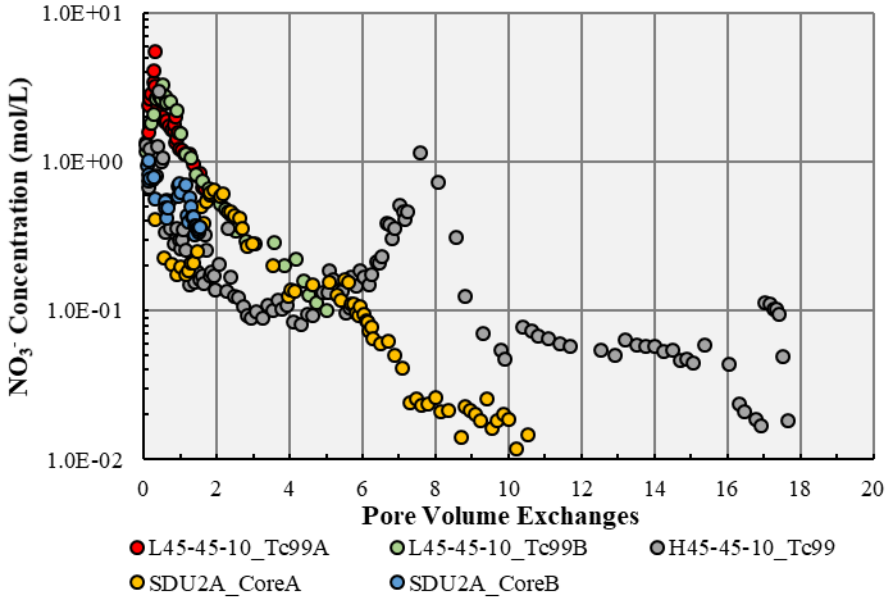

Figure 24. Cumulative percent nitrate (NO_3^-) released from DLM effluent

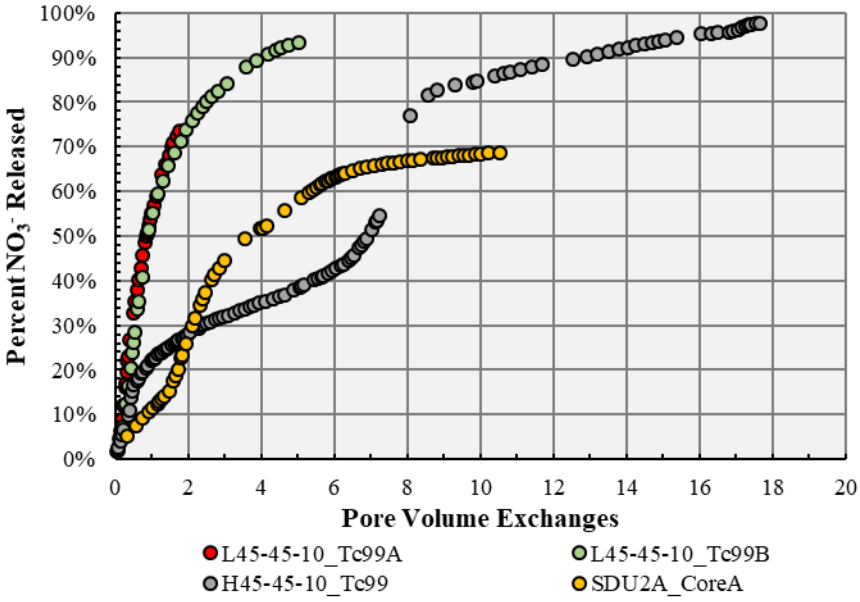

Figure 25. Effluent concentrations for L45-45-10_Tc99 A and B samples

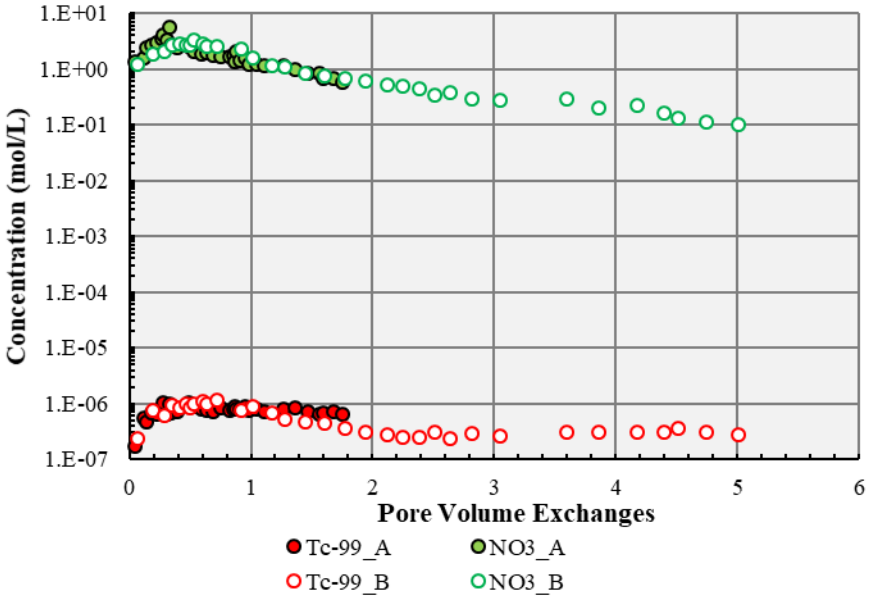

Figure 26. Cumulative percent released for L45-45-10_Tc99 A and B samples

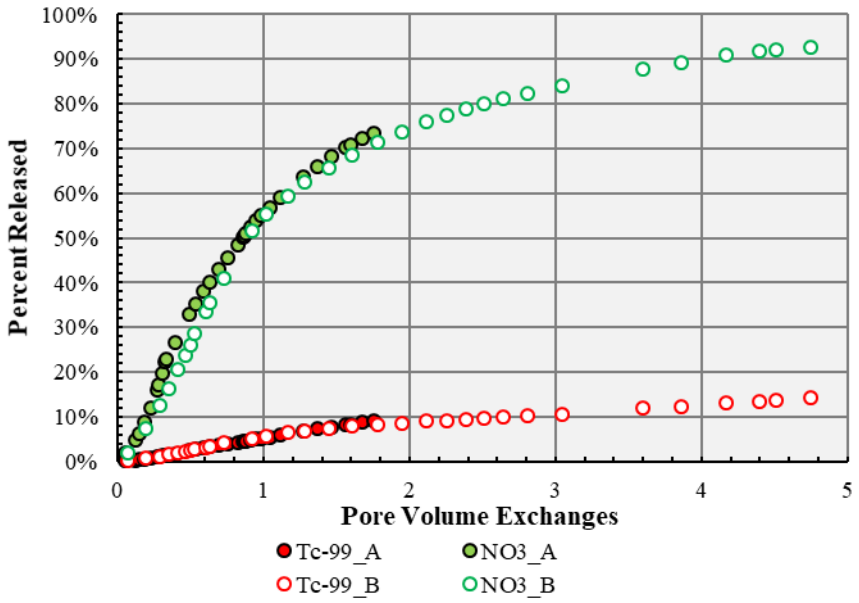

Figure 27. Effluent concentrations for SDU2A_Core A and B samples

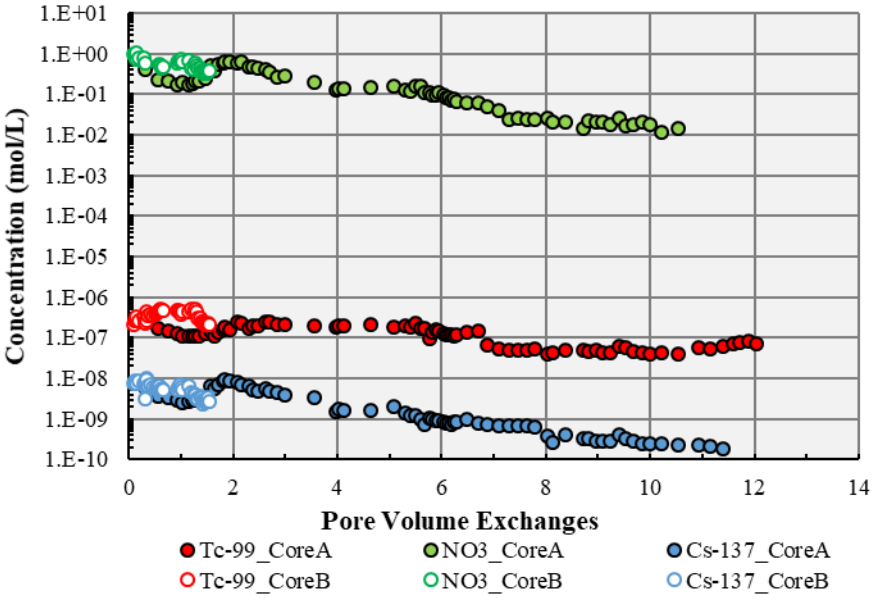

Figure 28. Cumulative percent released for SDU2A_Core A and B samples

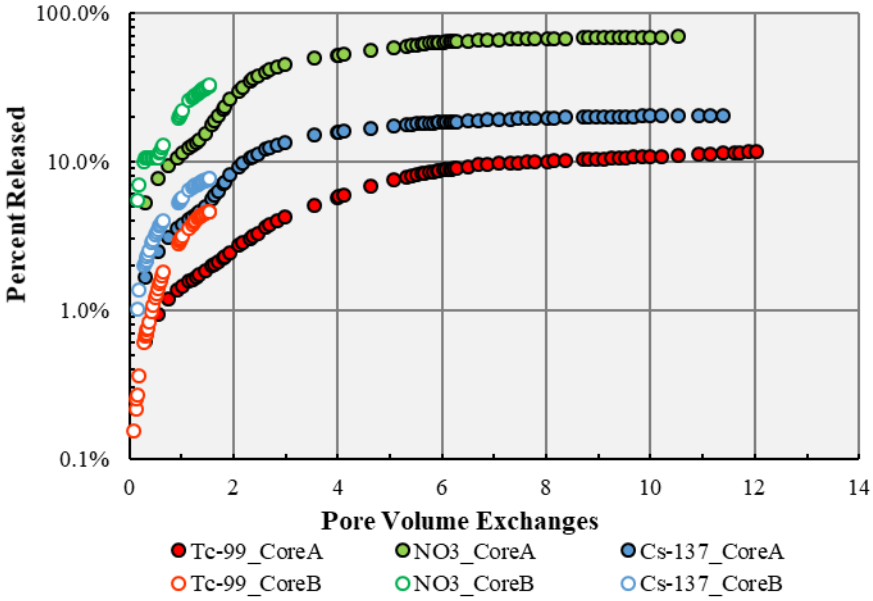

Figure 29. Tc-99 concentration in DLM effluent vs. pH

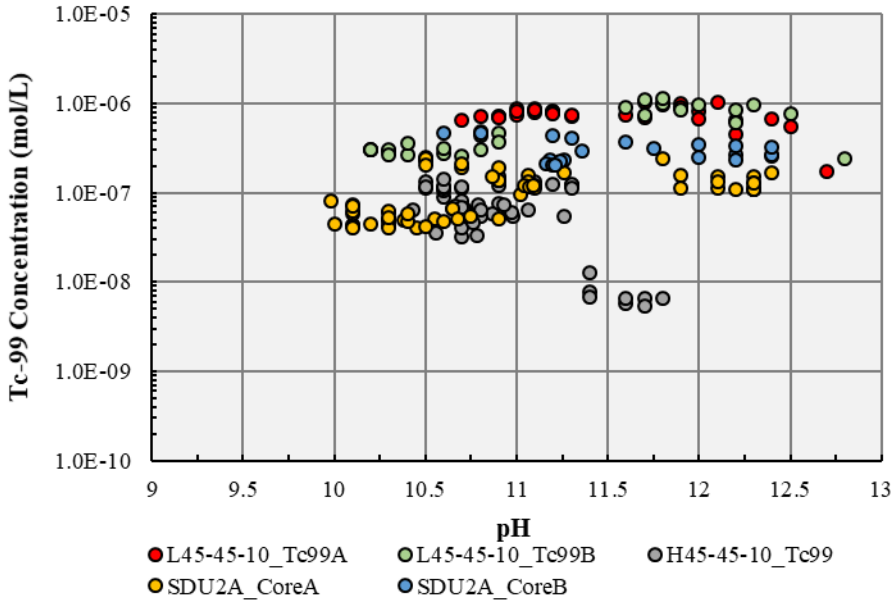

Figure 30. pH vs. pore volume exchanges

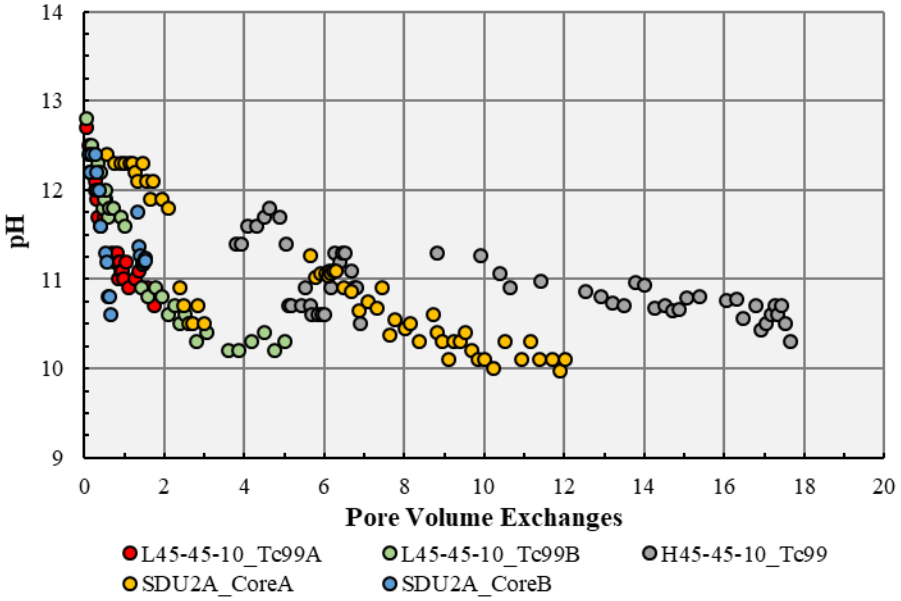

Figure 31. DLM effluent concentrations of Tc-99 vs. E_h (mV)

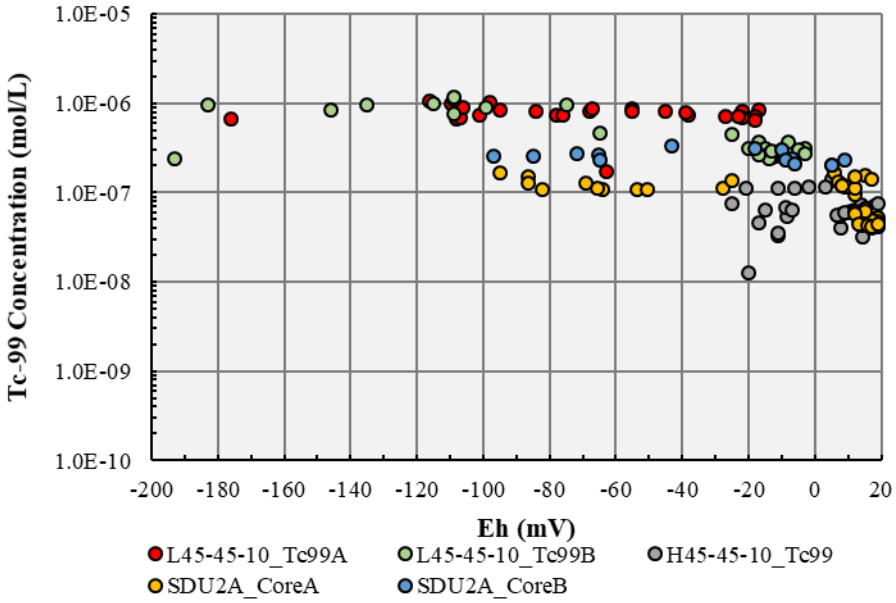

Figure 32. Eh (mV) vs. pore volume exchanges

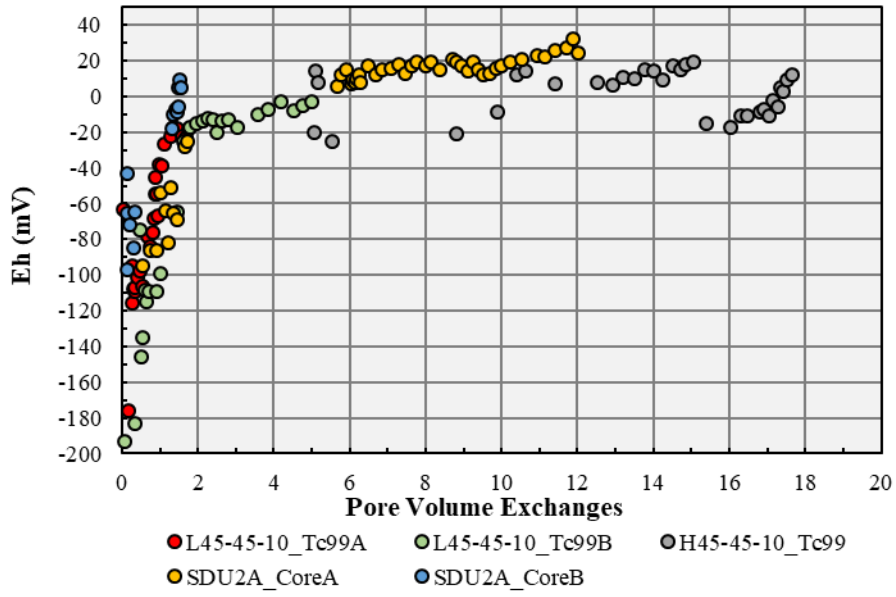

8.2.2 *I-129 DLM Experiments*

Figure 33. I-129 effluent concentrations for L45-45-10_I129 A and B samples

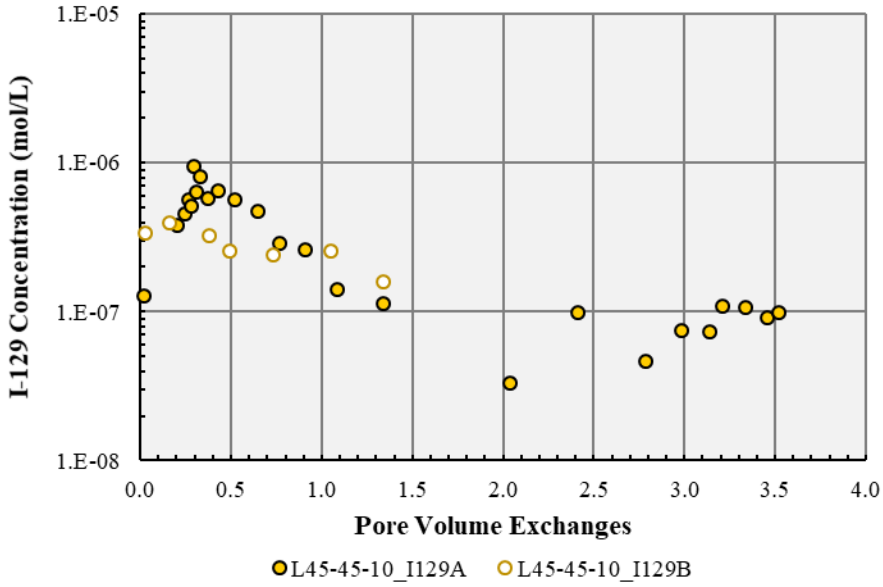

Figure 34. Cumulative percent I-129 released for L45-45-10_I129 A and B samples

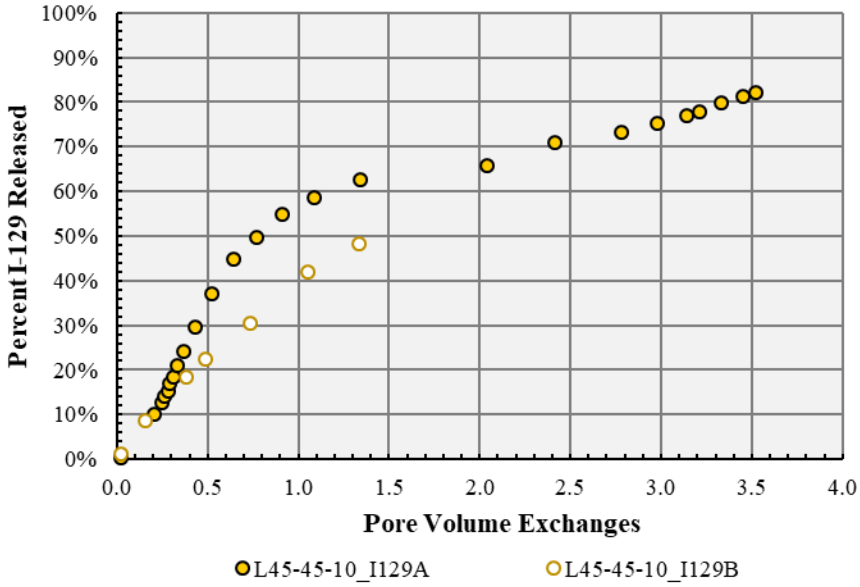

8.2.3 *Flow Measurements for DLM Experiments*

Figure 35. Hydraulic conductivity (K_{sat}) measured from DLM experiments

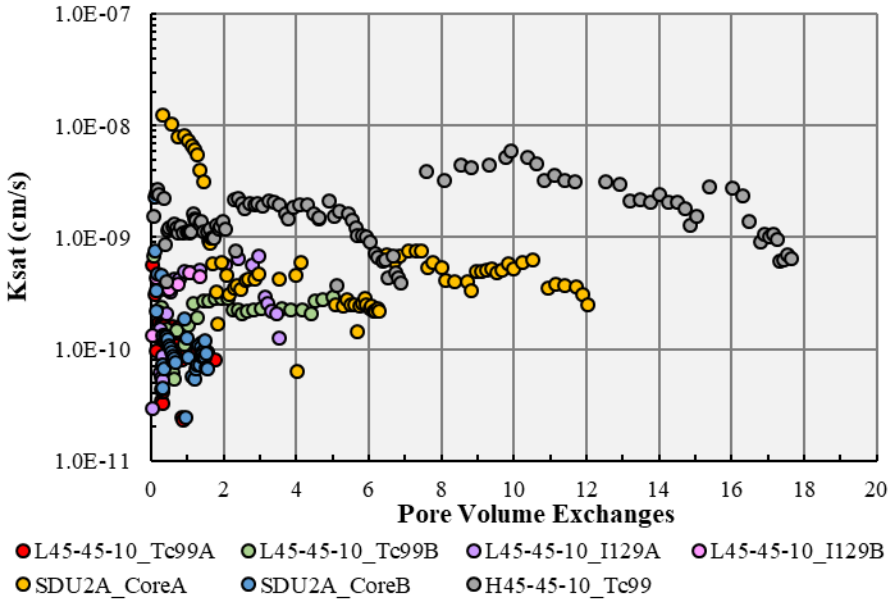

Figure 36. Hydraulic conductivity (K_{sat}) measured from DLM experiments categorized by sample type (field vs. lab synthesized). Lab synthesized samples are sub-categorized by slag type (i.e., Holcim vs. LeHigh).

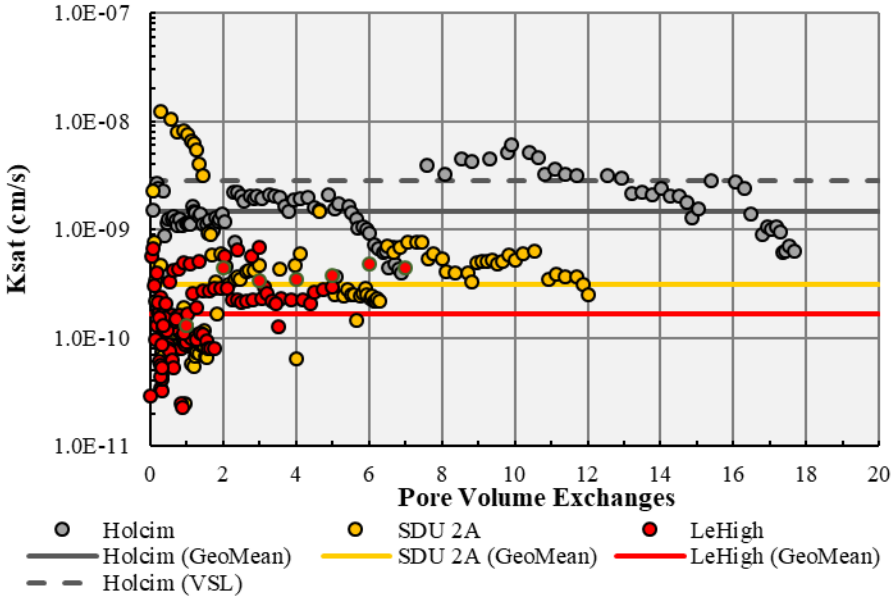

Note that in Figure 36, "GeoMean" is the geometric mean of K_{sat} values measured from DLM experiments for a given category (i.e., saltstone simulants using Holcim slag, saltstone simulants using LeHigh slag, or SDU 2A core samples). "Holcim (VSL)" is the K_{sat} measured by Vitreous State Laboratory (VSL) for a 45-45-10 saltstone simulant made using Holcim BFS (Gong et al., 2015).

Figure 37. Measured flow rate in units of pore volumes per year (PV/yr) for DLM experiments. Lines denote weighted average flow rate for a given DLM experiment. Line corresponds to the data points of the same color.